Epigenetic inactivation of miR-203 as a key step in neural crest epithelial-to-mesenchymal transition

Estefanía Sánchez-Vásquez[1], Marianne E. Bronner[2], Pablo H. Strobl-Mazzulla[1*]

[1]Laboratory of Developmental Biology, Instituto Tecnológico de Chascomús (CONICET-UNSAM), Chascomús 7130, Argentina

[2]Division of Biology 139-74, California Institute of Technology, Pasadena, CA 91125

[*]email: strobl@intech.gov.ar

Correspondence should be addressed to PHS-M

Key words: EMT, neural crest, miR-203, Snail2, DNA methylation, Phf12, migration

Summary statement

The EMT is a highly conserved process, involving similar levels of regulation in both neural crest and cancer cells. Our work shows an epigenetic-miRNA-gene regulatory circuit, conserved in cancer, which controls the timing of neural crest EMT as well.

Abstract

miR-203 is a tumor-suppressor microRNA with known functions in cancer metastasis. Here, we explore its normal developmental role in the context of neural crest development. As neural crest cells undergo an epithelial-to-mesenchymal transition to emigrate from the neural tube, miR-203 displays a reciprocal expression pattern with key regulators of neural crest delamination, *Phf12* and *Snail2*, and interacts with their 3'UTRs. Ectopic maintenance of miR-203 inhibits neural crest migration, whereas its functional inhibition using a "sponge" vector promotes premature neural crest delamination. Bisulfite sequencing further shows that epigenetic repression of miR-203 is mediated by the *de novo* DNA methyltransferase DNMT3B, whose recruitment to regulatory regions on the miR-203 locus is directed by SNAIL2 in a negative feedback loop. These findings reveal an important role for miR-203 in an epigenetic-microRNA regulatory network that influences the timing of neural crest delamination.

Introduction

Neural crest cells (NCC) are a transient embryonic cell population that arise in the neuroectoderm, then migrate to the periphery where they contribute to diverse derivatives including craniofacial bone and cartilage, neurons and glia of the peripheral nervous system, pigment cells, and portions of the cardiovascular system (Crane and Trainor, 2006). NCC emigrate from the forming central nervous system by undergoing an epithelial-mesenchymal transition (EMT), similar to that observed during initiation of tumor metastasis (Kerosuo and Bronner-Fraser, 2012). An evolutionarily conserved gene regulatory network (GRN) regulates NCC EMT and depends upon the coordinated action of transcription factors including *Snail1/2*, *Zeb2* (*Sip1*), and *FoxD3* (Simoes-Costa and Bronner, 2015). In addition to transcriptional regulators mediating neural crest EMT, epigenetic mechanisms including DNA methylation (Hu et al., 2012, Hu et al., 2014) and histone modifications (Strobl-Mazzulla and Bronner, 2012, Strobl-Mazzulla et al., 2010) are also at play. In particular, a repressor complex, comprised of SNAIL2 and the epigenetic reader PHF12 represses *cadherin 6b (Cad6b*) (Strobl-Mazzulla and Bronner, 2012), whose down-regulation is required for initiation of neural crest delamination from the neural tube. These results demonstrate an additional level of fine tuning and important role for epigenetic regulators during neural crest EMT, raising the intriguing possibility that other yet to be identified factors may be involved.

In recent years, microRNAs (miRNAs) have been shown to be key regulators of EMT in several tumor cells (Diaz-Lopez et al., 2014, Ding, 2014, Xia and Hui, 2012). MicroRNAs are ~22-nucleotides single-stranded RNAs that negatively regulate gene expression post-transcriptionally (Kloosterman and Plasterk,

2006) by inhibiting translation and/or causing degradation by binding to complementary sequences located at the 3'-untranslated region (3'-UTR) of target mRNAs. Approximately 50% of miRNAs genes are embedded or associated with CpGs islands, and their expression is most often regulated by methylation of cytosines therein (Weber et al., 2007). In several tumor cells, it has been shown that hypermethylation of anti-tumoral miRNAs leads to initiation of EMT (Ahmad et al., 2014, Kiesslich et al., 2013, Lujambio et al., 2008, Wang et al., 2012, Bonnomet et al., 2010, Diaz-Lopez et al., 2014, Ding, 2014, Nelson and Weiss, 2008, Xia and Hui, 2012). The commonalities between the migration of cancer cells and embryonic neural crest cells (Mayor and Theveneau, 2013, Scarpa and Mayor, 2016, Friedl and Gilmour, 2009) suggest the intriguing possibility that similar epigenetic-microRNA to those functioning in metastasis may be involved in NCC development. As case in point, we describe in avian embryos that the epigenetic repression of miR-203, directed by SNAIL2 enables upregulation of two of its direct targets, *Phf12* and *Snail2*, necessary for the delamination of the neural crest from the neural tube. These findings support the idea that a single microRNA, regulating key genes of the EMT process, may "throw" a precise switch mediating an epithelial to a mesenchymal state of neural crest cells.

Results

miR-203 expression is reduced at the time of NCC delamination

Given that *Phf12* and *Snail2* are involved in regulation of NCC EMT (Strobl-Mazzulla and Bronner, 2012), we performed an *in silico* and literature analysis to investigate miRNAs that might regulate these transcription factors. Interestingly, we found 9 and 7 families, respectively, of miRNAs in the 3'UTRs

of *Phf12* and *Snail2* with sites conserved across vertebrates (Table S1). Based on its their reported functionality, demonstrated target genes and expression pattern during chick development (Darnell et al., 2006), we further focused on miR-203 for in depth analysis. Importantly, miR-203 has been described to act as tumor suppressor (Benaich et al., 2014, Miao et al., 2014, Zhu et al., 2013b), that directly regulates *Snail2* expression (Gao et al., 2017, Shi et al., 2015, Zhang et al., 2015, Xiao et al., 2017), whose epigenetic repression causes metastasis in several tumor cells including NCC-derived melanoma (Boldrup et al., 2012, Boll et al., 2013, Chen et al., 2012, Chiang et al., 2011, Ding et al., 2013, Furuta et al., 2010, Huang et al., 2014, Ju et al., 2014, Moes et al., 2012, Zhang et al., 2014, Zhao et al., 2013, Bu and Yang, 2014, Lohcharoenkal et al., 2018). Moreover, the mature miR-203 sequence is highly conserved throughout vertebrates including the basal lamprey (Fig. 1B), suggesting an ancient and conserved function.

As a first step in analyzing its possible function during NCC development, we examined the expression pattern of miR-203 transcripts by *in situ* hybridization (ISH) in early chick embryos. By using LNA-DIG labelled probes, we found that mature miR-203 expression begins during gastrulation by stage 4 (Fig. S1A). During neurulation at the 1-4 somite stage (ss), miR-203 is consistently expressed in the forming neural tube (Fig. 1A). Interestingly, we observed a clear reduction by the 5 to 8ss in the miR-203 expression in the cranial neural tube, corresponding to the initiation of neural crest emigration. Analyses by stem-loop RT-qPCR confirmed that mature miR-203 expression is reduced from 5 to 6ss, coincident with the increase of *Snail2* and *Phf12* expression at the time

of NCC delamination (Fig. 1C). These results are consistent with the intriguing possibility that miR-203 has an important role in neural crest EMT.

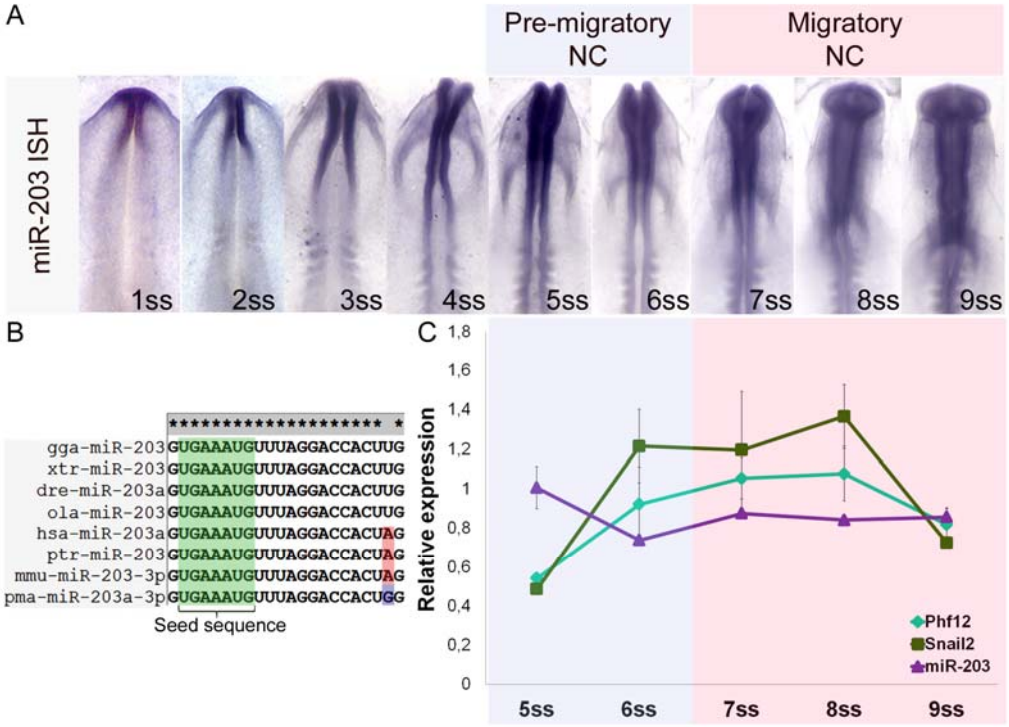

Figure 1: miR-203 expression is reduced at the time of NCC delamination. (A) Whole-mount *in situ* hybridization (ISH) using LNA-DIG labelled probes reveals a specific expression of the mature miR-203 on the neural tube which is reduced from 5 somite stage (ss) to 9ss. (B) Conservation analysis of miR-203 in vertebrates. Gga (*Gallus gallus),* xtr (Xenopus tropicalis), dre (*Danio* rerio), ola (*Oryzias* latipes), hsa (*Homo* sapiens), ptr (*Pan* troflodytes), mmu (*Mus* musculus), pma (*Petromyzon marinus).* (C) RT-qPCR analyses show reducing miR-203 expression from 5 to 6ss in an opposite manner than the observed increase on *Snail2* and *Phf12* expression at the beginning of NCC delamination.

miR-203 locus is highly methylated on pre-migratory NCC

In several metastatic tumor cells, the miR-203 locus is epigenetically silenced by DNA methylation (Chim et al., 2011a, Chim et al., 2011b, Diao et al., 2014, Furuta et al., 2010, Huang et al., 2014, Taube et al., 2013, Zhang et al., 2013, Zhang et al., 2011). Interestingly, we found by *in silico* analysis that the miR-203 locus is embedded in a CpG island (Fig. 2A). On this basis, we selected two genomic regions, one at the putative proximal promoter (region 1) and the other at the beginning of the pri-miR-203 (region 2), to analyze the DNA methylation abundance on pre-migratory (PM-NCC) or migratory (M-NCC) neural crest cells and the ventral neural tube (NT). By using bisulfite conversion, we observed high enrichment on methylated CpGs in region 2, but not on region 1, in the PM-NCC compared with the low abundance detected on the M-NCC and NT (Fig. 2B-C). These significant differences are clearly evident when comparing the total percentage of methylated CpGs (Fig. 2D-E) from the different samples. We identified that 18.4% and 28.9% of the CpGs are methylated on region 1 and 2 on PM-NCC, compared with 9.5% and 6.1% on the NT, and 5.3% and 7% detected on the M-NCC, respectively. These results suggest that the decreased expression of miR-203 in pre-migratory NC may be the consequence of hypermethylation of its locus.

DNMT3B and SNAIL2 are required for miR-203 methylation

De novo DNA methyltransferases DNMT3A and 3B are both involved in neural crest development (Hu et al., 2012). To examine the possibility that DNA methylation may be involved in regulating miR-203 expression, we examined the effects of loss of DNMT3A and 3B on miR-203 expression. To this end, we performed bisulfite sequencing after loss of function experiments with previously characterized fluorescein-tagged morpholino oligonucleotides, DNMT3A-MO

and DNMT3B-MO (Hu et al., 2012, Hu et al., 2014). After unilateral injection and electroporation, dorsal neural tubes from 6ss embryos were dissected and bisulfite converted to analyze the methylation abundance on region 2 of miR-203 locus (Fig. 2A). The results show that loss of function of either of the two DNMTs consistently decreases the abundance of methylated CpGs in the region 2 (Fig. 2F). However, depletion of DNMT3B, but not DNMT3A, resulted in significant differences in methylation of miR-203.

Transcription factors specifically bind to target DNAs to recruit and guide DNA methyltransferases to specific genomic sites (Siegfried and Simon, 2010). During tumor metastasis, SNAIL2 binds to the miR-203 promoter to inhibit its transcription (Ding et al., 2013), though the mechanism underlying this repression is unknown. Our bioinformatic analysis reveal several SNAIL2-binding sites ~1kb upstream of the pre-miR-203 (Fig. 2A, Table S2), two of which have a high binding score (>9) accordingly to JASPAR 2018 (http://jaspar.genereg.net/). To test the effects of SNAIL2 loss of function, we electroporated a previously characterized Snail2 morpholino (Snail2-MO) (Taneyhill et al., 2007) unilaterally and dissected half dorsal neural tubes from 6ss embryos for analysis of miR-203 expression and DNA methylation. Interestingly, the results show that Snail2 knockdown causes a significant upregulation of miR-203 expression (Fig. 2G). Consistent with this finding, we found a significant reduction in the abundance of methylated CpGs in region 2 of the miR-203 locus (Fig. 2H). These results suggest that SNAIL2 is involved in the epigenetic repression of miR-203 in the premigratory neural crest.

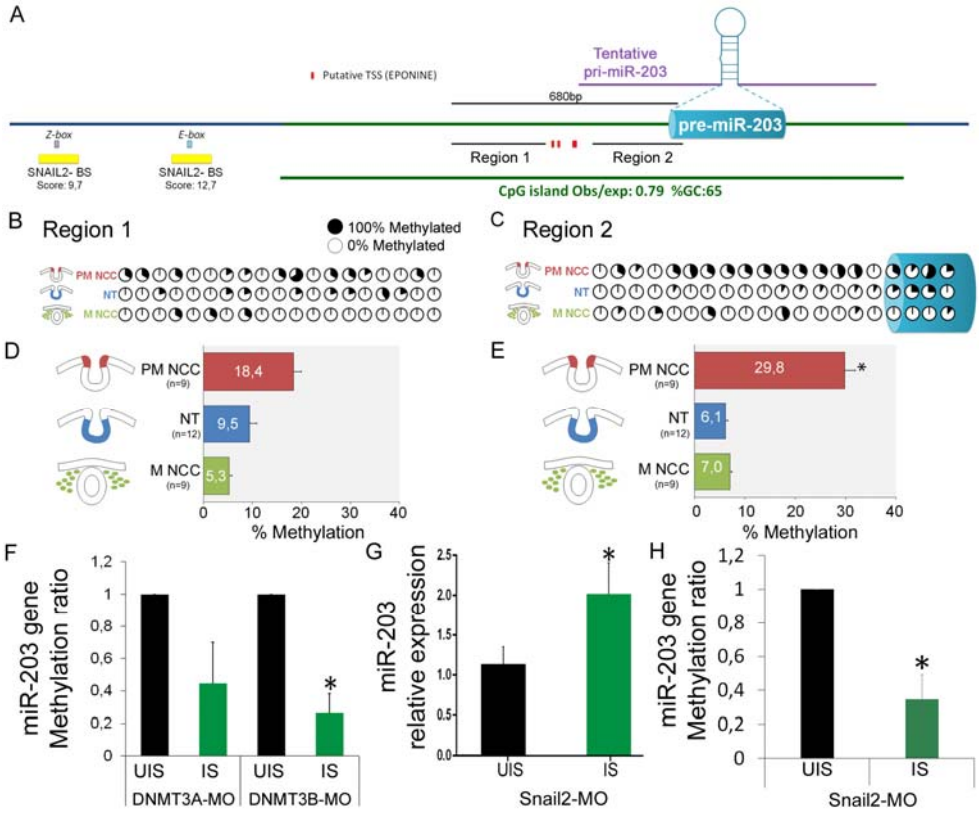

Figure 2: *SNAIL2 and DNMT3B are required for DNA* methylation on miR-203 locus on premigratory NCC. (A) miR-203 genomic context. The CpG island content (green bar) for miR-203 gene was identified using the UCSC genome browser (https://genome.ucsc.edu/) and Ensembl (http://www.ensembl.org/). The putative transcriptional start sites (TSS) were obtained using Eponine (https://www.sanger.ac.uk/science/tools/eponine). The putative binding sites for SNAIL2 were mapped using JASPAR 2018 (http://jaspar.genereg.net/). We also show the two regions used in our bisulfite sequencing and the pre-miR-203 accordingly to the miRbase (http://www.mirbase.org/). Bisulfite sequencing profiles of CpGs methylation on the region 1 (B) and region 2 (C) were analyzed on pre-migratory NCC (PM-NCC), migratory NCC (M-NC), and ventral neural tube (NT). Percentage of each methylated CpG sites are shown with filled (100% methylated) and open (0% methylated) circles. Bar graph represent the total percentages of methylated CpGs on the different regions for the three analyzed samples on the region 1 (D) and the region 2 (E). We evidenced in PM-NCC a higher percentage of methylated CpGs compared with the other samples. Number in brackets indicated the analyzed sequences. Asterisk (*) indicate significant differences by ANOVA. (F) Morpholino-mediated loss of DNMT3A (DNMT3A-MO) and DNMT3B (DNMT3B-MO) function results in a reduction of

197 methylated CpGs on the injected side (IS) compared with the uninjected side (UIS) of the same
198 group of embryos. Morpholino-mediated loss of SNAIL2 (SNAIL2-MO) function maintains an
199 elevated level of miR-203 expression (G) and reduced CpGs methylation on the region 2 (H) on
200 the IS compared with the UIS of the same group of embryos. Asterisk (*) indicate significant
201 differences by Student's *t*-test.
202
203 *Overexpression of miR-203 causes loss of migrating NCC*
204 Since miR-203 expression is epigenetically repressed at the initiation of their
205 migration, we asked whether maintenance of miR-203 expression would
206 prevent neural crest delamination. To this end, we designed an overexpression
207 vector in which we cloned the pre-miR-203 sequence, plus a few hundred base
208 pair arms for correct processing, under the control of CAG promoter (pCAG-
209 203) (Fig. 3A). Overexpression of miR-203 in pCAG-miR-203 electroporated
210 embryos was confirmed by LNA-ISH (Fig. S2B). To demonstrate that the pCAG-
211 miR-203 expresses a functional miR-203, we first used a two-colored sensor
212 vector (Cao et al., 2007) comprised of a nuclear-localized destabilized EGFP
213 with a half-life of 4 hours (d4EGFP$_N$), driven by a CAG promoter, followed by a
214 3'UTR containing two copies of a bulged complementary sequence for miR-203.
215 In addition, the vector contains a nuclear-localized monomeric red fluorescent
216 protein (mRFP$_N$) driven by another CAG promoter that serves as an
217 electroporation control (see scheme of pSdmiR-203 in figure S2C). Together
218 with the dual sensor pSdmiR-203, we co-electroporated either control empty
219 vector (left) or the vector expressing miR-203 (right) onto each side of the
220 embryo (Fig. S2D). The results show that on the control side, most of the
221 electroporated cells appeared yellow, due to expression of d4EGFP$_N$ and
222 mRFP$_N$. However, on the experimental side, overexpression of miR-203 causes

223 a strong reduction of d4EGFP$_N$ and the cells only express mRFP$_N$ (Fig. S2E).
224 These results confirm the functionality of our miR-203 expression construct.
225 Gain-of-function experiments were conducted by electroporating the miR-203
226 vector on one side of the embryo (Fig. S2A). The results show that miR-203
227 overexpression causes a drastic reduction in the numbers of migratory neural
228 crest cells identified by *Sox10* expression (Fig. 3B). By categorizing embryos
229 according to their phenotype (normal or reduced migratory NCC), we observed
230 a significant increase in the number of embryos with a reduced number of
231 migratory NCC on pCAG-203 electroporated side compared with control
232 embryos electroporated with an empty vector (pCAG) (Fig. 3C). To rule out the
233 possibility that this may be secondary to a specification defect, we analyzed the
234 expression of early neural crest specifier genes by immunohistochemistry at
235 pre-migratory stages. Interestingly, our results demonstrate that overexpression
236 of miR-203 does not affect expression of FOXD3, one of earliest neural crest
237 specification markers (Fig. 3D), suggesting that specification occurs normally. In
238 contrast, there was a clear reduction in SNAIL2, demonstrating reciprocal
239 repression. Taken together, our results highlight the role of miR-203 in NCC
240 delamination, likely by affecting EMT inducers like SNAIL2.

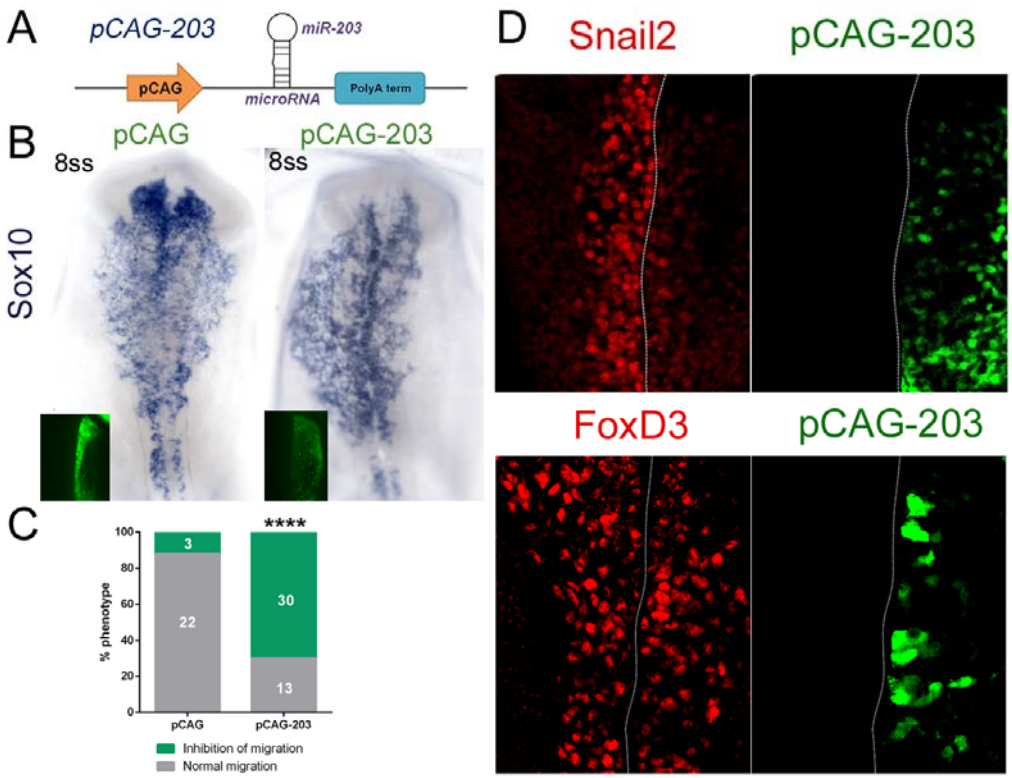

Figure 3: miR-203 overexpression prevents NCC delamination without affecting specification. (A) Scheme of pCAG-203 vector to overexpress miR-203. (B) *In situ* hybridization for *Sox10* showed inhibition of NCC migration in the pCAG-203 injected side, in comparison with the uninjected side of the same embryos and with embryos injected with an empty pCAG vector. (C) Quantitation of the embryos according to their phenotypes (normal migration versus inhibition of migration) was analyzed. Numbers in the graphs represent the numbers of analyzed embryos. ****P < 0,0001 by contingency table followed by X^2 test. (D) Immunohistochemistry analyzes on miR-203 overexpressing embryos evidenced a reduced expression of SNAIL2 but does not affect the expression of the early NCC specifier FOXD3.

Loss of miR-203 function causes premature NCC delamination

Given that miR-203 is epigenetically repressed in pre-migratory NCC and overexpression of miR-203 causes defect in their delamination, we next asked if early loss of miR-203 function would result in premature neural crest

delamination. To test this possibility we adapted a protocol (Kluiver et al., 2012) to generate a “sponge” vector containing repeated miR-203 antisense sequences (pSmiR-203) to sequester endogenous miR-203 (Fig. 4A). A sponge vector containing a scrambled sequence (pSmiR-scramble) was designed as a control. As predicted, electroporation of pSmiR-203 resulted in premature NCC migration, when compared with the contralateral uninjected side, analyzed by immunohistochemistry for SNAIL2 and FOXD3, or by ISH for *Sox10* (Fig. 4B). Importantly, no difference in timing of delamination was observed after electroporation of the pSmiR-scramble. By categorizing embryos according to their phenotype, premature versus normal migration, we observed a significant difference in percentage of embryos exhibiting premature NCC migration in pSmiR-203 electroporated embryos (Fig. 4C). Notably, reduction of miR-203 function altered not only initiation of NCC delamination, but also shortened the overall length of time during which delamination occurred (Fig. 4D-D’). This is based on the observation that on the side injected with pSmiR-203, all the Sox10+ NCCs have completed their delamination, compared with the contralateral side where many premigratory neural crest cells still persist on the dorsal neural tube. These results clearly confirm that miR-203 controls the temporal regulation of NCC delamination.

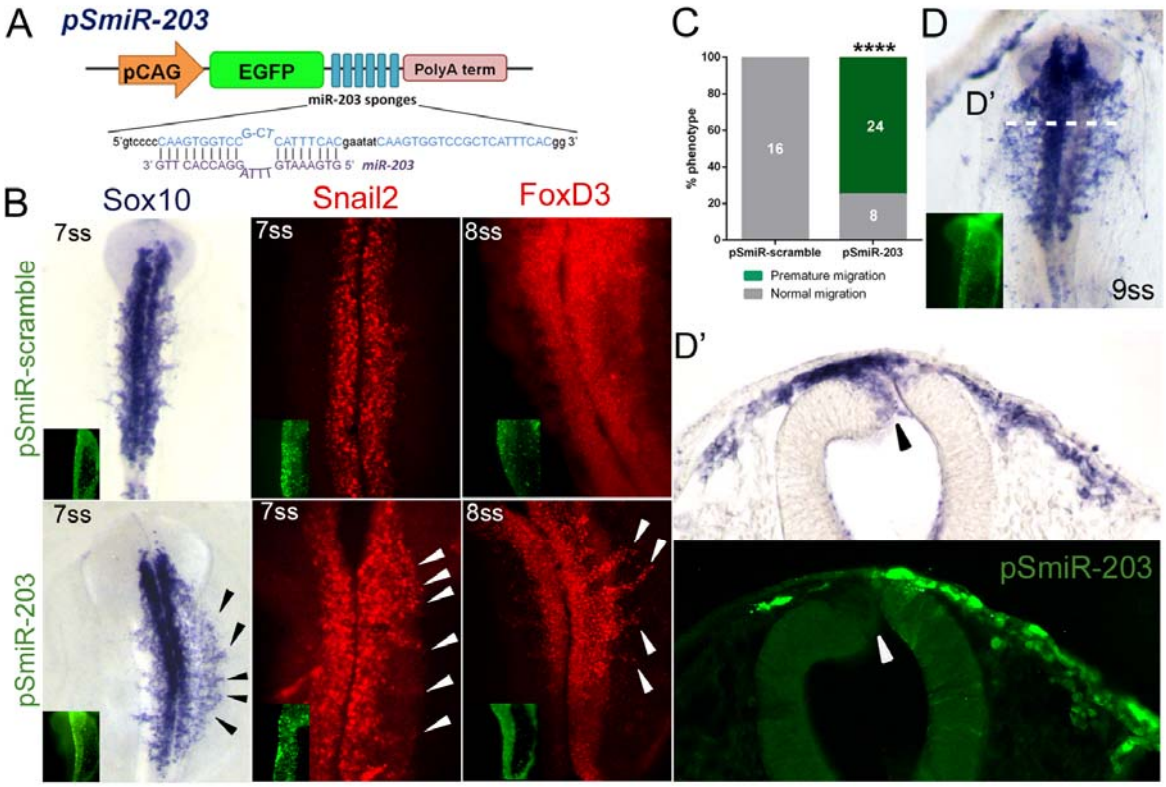

Figure 4: miR-203 sponge vector causes premature NCC delamination. (A) Scheme of pSmiR-203 sponge vector having a bulged miR-203 antisense sequences downstream of the EGFP reporter. (B) Electroporated embryos with pSmiR-203 causes premature migration of NCC evidenced by *in situ* hybridization for Sox10 and immunohistochemistry for SNAIL2 and FOXD3, and compared with the uninjected side of the same embryos or injected with pSmiR-scramble vector. Arrowhead indicated premature migratory neural crest cells. (C) Quantitation of pSmiR-203 or pSmiR-scramble treated embryos according to the observation of premature NCC migration. Numbers in the graph represent the analyzed embryos. ****P<0,0001 by contingency table followed by X^2 test. (D-D') Neural crest cells from the sponge injected site complete their delamination in advance compare with the uninjected site where many *Sox10* expressing cells are still on the neural tube (see black arrowhead).

miR-203 targets the 3'UTRs of Snail2 and Phf12

To test whether *Snail2* and *Phf12* genes are direct targets of miR-203, we designed two-colored sensor vectors in which we cloned, downstream of the

pCAG and d4EGFP$_N$, the 3'UTRs containing the wild (pUTR-Snail2/Phf12) or mutated (pUTR-mutSnail2/Phf12) miR-203 binding sites (Fig. 5A). Co-electroporation of these vectors (Fig. 5B) demonstrated that overexpression of miR-203 specifically inhibited d4EGFP$_N$ expression when it was fused to the 3'UTRs of *Snail2* and *Phf12* but was uniformly distributed when miR-203 binding sites were mutated (Fig. 5C-D). These results confirm that *Snail2* and *Phf12* are endogenous targets of the same microRNA, miR-203.

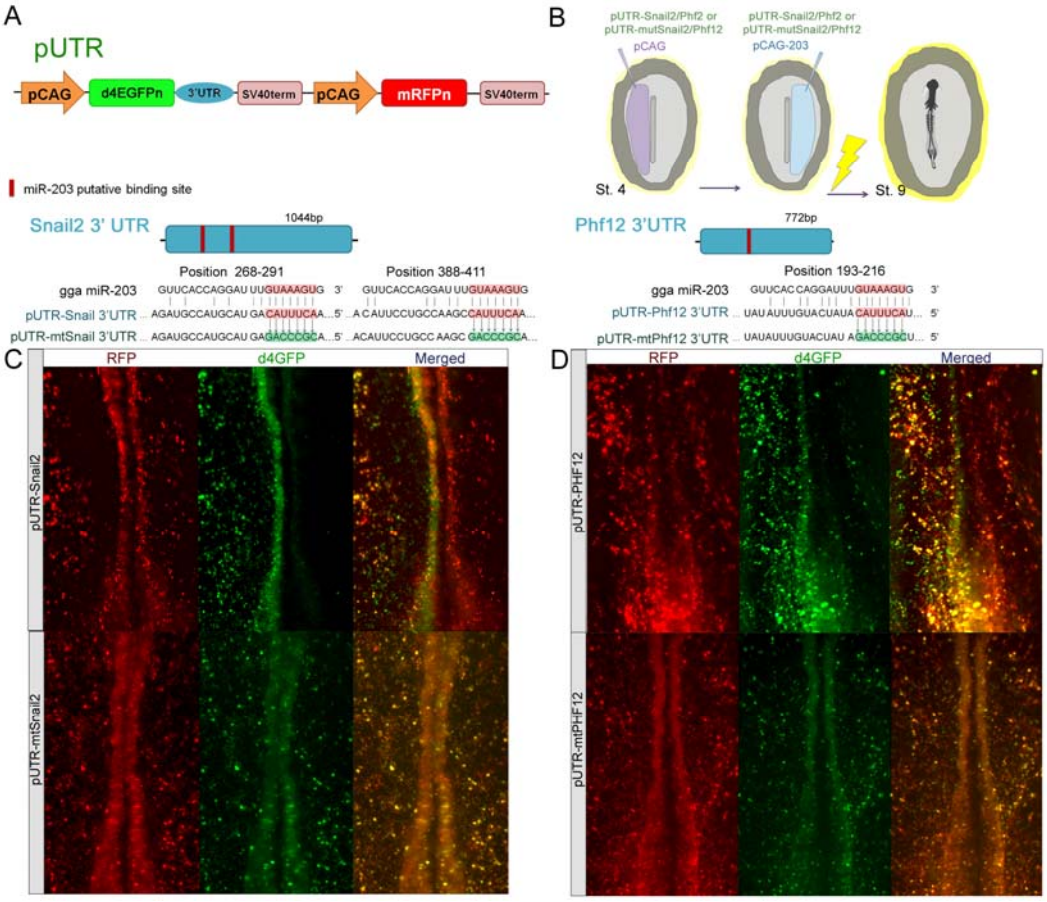

Figure 5: *Snail2* and *Phf12* 3'UTRs are direct targets of miR-203. (A) Scheme of dual colored sensor vector containing wild or mutated (mt) 3'UTRs from Snail2 (pUTR-Snail2) and Phf12 (pUTR-Phf12*)*. pCAG, Chick β-actin promoter; d4EGFP$_N$ nuclear-localized destabilized EGFP with a half-life of 4 h; mRFP$_N$, nuclear-localized monomeric red fluorescent protein. (B) Diagram of electroporation assays for 3'UTR-sensor experiments. Electroporation of sensor

vector containing the 3'UTRs for (C) *Snail2* (pUTR-Snail2) or (D) *Phf12* (pUTR-Phf12) together with miR-203 overexpressing vector (pCAG-203) causes a consistent reduction on the d4EGFP$_N$ expression (right side) compared with the control side (left side). Mutation of miR-203-binding sites in the 3'UTRs of *Snail2* (pUTR-mtSnail2) or *Phf12* (pUTR-mtPhf12) caused that most of the electroporated cells were yellow, expressing both d4EGFP$_N$ and mRFP$_N$, even when miR-203 is overexpressed (right side).

Discussion

There is accumulating evidence for the importance of microRNAs in normal development as well as in several diseases, including tumor metastasis. Our study highlights the key role of a single microRNA, miR-203, in regulating the timing to initiation of the EMT program in neural crest cells. The results show that repression of miR-203 occurs via high levels of DNA methylation of the miR-203 locus by the DNMT3B, whose specific activity is directed by SNAIL2. In this scenario, repression of miR-203 is directed by SNAIL2 in a feedback-loop that enables expression of two direct targets of miR-203, *Phf12* and *Snail2*, which in turn are necessary for neural crest delamination. Finally, miR-203 gain- and loss-of-function cause reduction or premature NCC delamination, respectively. Taken together, the results reveal for the first time an epigenetic-miRNA-gene regulatory circuit that controls the timing of neural crest delamination (Fig. 6A). These findings support the idea that a single microRNA may "throw the switch" from an epithelial to a mesenchymal state in the neural crest and thus stabilize the core gene regulatory networks in these two states.

There is increasing evidence to suggest that miRNAs often act as fine-tuning regulators rather than as primary gene regulators (Hornstein and Shomron, 2006). Accordingly, we postulate that miR-203 may act by shifting the levels of

SNAIL2 and PHF12 to prevent premature NCC delamination. A similar epigenetic-miRNA control of the core transcription factors necessary for EMT (EMT-TFs) has been also described in cancer cells (Wright et al., 2010, Guttilla et al., 2012, Xia and Hui, 2012, Kiesslich et al., 2013, Ding, 2014). Interestingly, some miRNAs and EMT-TFs form a tightly interconnected feedback loop that controls epithelial cell plasticity (Moes et al., 2012, Ding, 2014, Wellner et al., 2009), similar to our observation that SNAIL2 directs the epigenetic repression of miR-203. These feedback-loops provide self-reinforcing signals and robustness to maintain the epithelial or mesenchymal cell state in response to different environmental cues. miR-203 is highly conserved from lamprey to human and appears to be an evolutionary novelty in vertebrates (Heimberg et al., 2010). Our data demonstrate that miR-203 is a key regulator of NCC delamination by a reversible epigenetic-miRNAs. Given that the EMT program is a highly conserved process, involving similar transcription factors in both embryonic and cancer cells, these finding open new avenues for understanding normal and pathological development, as well as tumor metastasis.

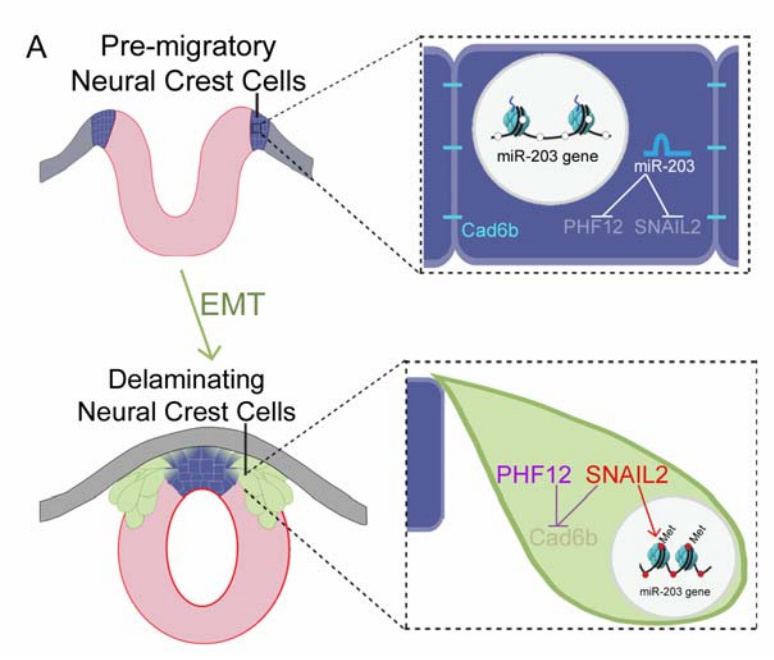

Figure 6: Hypothetical model. Our results show that during NCC specification, miR-203 is highly expressed and preventing the initial accumulation of SNAIL2 and PHF12. Previous to NCC delamination, the accumulation of SNAIL2 causes the epigenetic silencing, mediated by DNMT3B, of miR-203. Then, the lack of miR-203 allows a rapid upregulation of both *Snail2* and *phd12* at the same time, which are necessaries for Cad6b repression at the beginning of the NCC epithelial-to-mesenchymal transition.

Materials and methods

RNA preparation and RT-qPCR

RNA was prepared from individual embryos (n=6) using the isolation kit RNAqueous-Micro (Ambion) following the manufacturer's instruction. The RNA was treated with amplification grade DNaseI (Invitrogen) and then reversed transcribed to cDNA with a reverse transcription kit (SuperScript II; Invitrogen) using stem-loop-miRNA-specifics (Chen et al., 2005) primers and random hexamers. QPCRs were performed using a 96-well plate qPCR machine (Stratagen) with SYBR green with ROX (Roche). Normalization controls genes

for qPCR were: for miR-203, miR-16 (Lardizabal et al., 2012) and for *Snail2* and *Phf12*, *Hprt1* (Simoes-Costa and Bronner, 2016). For a complete list of primer see table S3.

Bisulfite sequencing

Samples were obtained by dissecting of 9 embryos at stage 6ss, for premigratory NCC (PM-NCC), dorsal neural tube, and ventral neural tube (NT). In addition, we dissected 13 embryos at stage 11-13ss to obtain the migratory NCC (M-NCC). For the morpholino-mediated loss of DNMT3A, DNMT3B and SNAIL2 experiment, eight dorsal neural tubes from the injected and uninjected sides were dissected. For a complete list of morpholinos see table S3. All the tissues were lysed and bisulfite-converted with the EpiTect Plus Bisulfite Conversion Kit (Qiagen) following the manufacturer's instructions. The regulatory regions of miR-203 were amplified by using two sets of nested primers (see table S3) from the bisulfite-converted DNA. The obtained products were gel-purified and cloned into the pGEM-T Easy Vector (Promega). Individual clones were sequenced and analyzed.

Electroporation

Chicken embryos were electroporated at stage 4-5 using previously described techniques (Sauka-Spengler and Barembaum, 2008). The vectors and morpholinos were injected by air pressure using a glass micropipette and platinum electrodes were placed vertically across the chick embryos and electroporated with five pulses of 5.5 V for 50 ms at 100 ms intervals. Embryos were cultured in 0.5 ml albumen in tissue-culture dishes until the desired

388 stages. Embryos were then removed and fixed in 4% PFA and used for
389 immunohistochemistry or *in situ* hybridization.
390
391 *In situ hybridization*
392 Whole-mount chick *in situ* hybridization for mRNAs and for microRNA was
393 performed as described previously (Acloque et al., 2008, Darnell et al., 2006).
394 LNA probe for miR-203 used in the assay were obtained from Exiqon and DIG-
395 labelled by using the DIG oligonucleotide 3' end labeling kit (Roche). After ISH,
396 some embryos were fixed in 4% PFA in PBS, washed, embedded in gelatin,
397 and cryostat sectioned at a thickness of 14–16 µm. They were photographed
398 using the NIS-Elements Advanced Research software (Nikon) with an Eclipse
399 E600 microscope (Nikon) and processed using Photoshop CS3 (Adobe).
400
401 *Immunohistochemistry*
402 Whole-mount chick immunohistochemistry was performed as described
403 previously (Taneyhill et al., 2007). Briefly, embryos were fixed for 15 min in 4%
404 PFA and then permeabilized and blocked in TBS (500 mM Tris-HCl, pH 7.4, 1.5
405 M NaCl, and 10 mM $CaCl_2$) containing 0.1% Triton X-100 (TBS-T) and 5% FBS
406 for 60 min at room temperature. Primary antibodies were diluted in TBS-T/FBS
407 and incubated overnight at 4°C. Primary antibodies used were mouse anti-
408 Snail2 (1:100), (1:100; supplied by the Developmental Studies Hybridoma
409 Bank), and rabbit anti-FoxD3 (1:300; gift of P. Labosky, Vanderbilt University
410 Medical Center, Nashville, TN). Secondary antibodies used were goat anti-
411 mouse and anti-rabbit Alexa Fluor 594 (1:500; all obtained from Molecular
412 Probes) diluted in TBS-T/FBS and incubated for 45 min at room temperature.

All washes were performed in TBS-T at room temperature. Some embryos were subsequently embedded in gelatin, cryostat sectioned at 12-16µm, photographed using the NIS-Elements Advanced Research software (Nikon) with an Eclipse E600 microscope (Nikon) and processed using Photoshop CS3 (Adobe).

MicroRNA sponge generation

Oligos designed to generate miR-203 sponge were ordered phosphorylated and PAGE purified at a 100 nmol scale (see table S2) and dissolved to 50 mM in STE buffer (100 mM NaCl, 10 mM Tris/HCL, 1 mM EDTA, pH 8.0). Sense and antisense oligos were mixed at a 1:1 ratio and annealed by incubation at 100°C for 10 minutes followed by slow cooling. The “sponge” vector was generated following previously described protocols (Kluiver et al., 2012).

Acknowledgments

We thank Dr. Xinwei Cao for the two-colored sensor vector, and Dr. Andrew Pollok for the advices on the design of sponge vector.

Competing interests The authors declare no conflicts of interest

Funding

This work was supported by the Fogarty International Center of the NIH (R21TW011224 to MEB and PHS-M) and the Agencia Nacional de Promoción Científica y Tecnológica (PICT 2016-0747 to PHS-M).

Author contributions

436 ESV, MEB and PHS-M conceived, designed and analyzed the experiments.

437 ESV performed all the experiments. ESV, MEB and PHS-M wrote the

438 manuscript.

439

440 **References**

441 Acloque, H., Wilkinson, D. G., & Nieto, M. A. (2008). In situ hybridization
442 analysis of chick embryos in whole-mount and tissue sections. *Methods*
443 *Cell Biol, 87*, 169-185. doi: 10.1016/S0091-679X(08)00209-4
444 Ahmad, A., Li, Y., Bao, B., Kong, D., & Sarkar, F. H. (2014). Epigenetic
445 regulation of miRNA-cancer stem cells nexus by nutraceuticals. *Mol Nutr*
446 *Food Res, 58*(1), 79-86. doi: 10.1002/mnfr.201300528
447 Benaich, N., Woodhouse, S., Goldie, S. J., Mishra, A., Quist, S. R., & Watt, F.
448 M. (2014). Rewiring of an epithelial differentiation factor, miR-203, to
449 inhibit human squamous cell carcinoma metastasis. *Cell Rep, 9*(1), 104-
450 117. doi: 10.1016/j.celrep.2014.08.062
451 Boldrup, L., Coates, P. J., Wahlgren, M., Laurell, G., & Nylander, K. (2012).
452 Subsite-based alterations in miR-21, miR-125b, and miR-203 in
453 squamous cell carcinoma of the oral cavity and correlation to important
454 target proteins. *J Carcinog, 11*, 18. doi: 10.4103/1477-3163.104007
455 Boll, K., Reiche, K., Kasack, K., Morbt, N., Kretzschmar, A. K., Tomm, J. M., . . .
456 Hackermuller, J. (2013). MiR-130a, miR-203 and miR-205 jointly repress
457 key oncogenic pathways and are downregulated in prostate carcinoma.
458 *Oncogene, 32*(3), 277-285. doi: 10.1038/onc.2012.55
459 Bonnomet, A., Brysse, A., Tachsidis, A., Waltham, M., Thompson, E. W.,
460 Polette, M., & Gilles, C. (2010). Epithelial-to-mesenchymal transitions
461 and circulating tumor cells. *J Mammary Gland Biol Neoplasia, 15*(2), 261-
462 273. doi: 10.1007/s10911-010-9174-0
463 Bu, P., & Yang, P. (2014). MicroRNA-203 inhibits malignant melanoma cell
464 migration by targeting versican. *Exp Ther Med, 8*(1), 309-315. doi:
465 10.3892/etm.2014.1708
466 Cao, X., Pfaff, S. L., & Gage, F. H. (2007). A functional study of miR-124 in the
467 developing neural tube. *Genes Dev, 21*(5), 531-536. doi:
468 10.1101/gad.1519207
469 Crane, J. F., & Trainor, P. A. (2006). Neural crest stem and progenitor cells.
470 *Annu Rev Cell Dev Biol, 22*, 267-286. doi:
471 10.1146/annurev.cellbio.22.010305.103814
472 Chen, C., Ridzon, D. A., Broomer, A. J., Zhou, Z., Lee, D. H., Nguyen, J. T., . . .
473 Guegler, K. J. (2005). Real-time quantification of microRNAs by stem-
474 loop RT-PCR. *Nucleic Acids Res, 33*(20), e179. doi: 10.1093/nar/gni178
475 Chen, H. Y., Han, Z. B., Fan, J. W., Xia, J., Wu, J. Y., Qiu, G. Q., . . . Peng, Z.
476 H. (2012). miR-203 expression predicts outcome after liver
477 transplantation for hepatocellular carcinoma in cirrhotic liver. *Med Oncol,*
478 *29*(3), 1859-1865. doi: 10.1007/s12032-011-0031-9
479 Chiang, Y., Song, Y., Wang, Z., Chen, Y., Yue, Z., Xu, H., . . . Liu, Z. (2011).
480 Aberrant expression of miR-203 and its clinical significance in gastric and

colorectal cancers. *J Gastrointest Surg, 15*(1), 63-70. doi: 10.1007/s11605-010-1367-8

Chim, C. S., Wan, T. S., Wong, K. Y., Fung, T. K., Drexler, H. G., & Wong, K. F. (2011). Methylation of miR-34a, miR-34b/c, miR-124-1 and miR-203 in Ph-negative myeloproliferative neoplasms. *J Transl Med, 9*, 197. doi: 10.1186/1479-5876-9-197

Chim, C. S., Wong, K. Y., Leung, C. Y., Chung, L. P., Hui, P. K., Chan, S. Y., & Yu, L. (2011). Epigenetic inactivation of the hsa-miR-203 in haematological malignancies. *J Cell Mol Med, 15*(12), 2760-2767. doi: 10.1111/j.1582-4934.2011.01274.x

Darnell, D. K., Kaur, S., Stanislaw, S., Konieczka, J. H., Yatskievych, T. A., & Antin, P. B. (2006). MicroRNA expression during chick embryo development. *Dev Dyn, 235*(11), 3156-3165. doi: 10.1002/dvdy.20956

Diao, Y., Guo, X., Jiang, L., Wang, G., Zhang, C., Wan, J., . . . Wu, Z. (2014). miR-203, a tumor suppressor frequently down-regulated by promoter hypermethylation in rhabdomyosarcoma. *J Biol Chem, 289*(1), 529-539. doi: 10.1074/jbc.M113.494716

Diaz-Lopez, A., Moreno-Bueno, G., & Cano, A. (2014). Role of microRNA in epithelial to mesenchymal transition and metastasis and clinical perspectives. *Cancer Manag Res, 6*, 205-216. doi: 10.2147/CMAR.S38156

Ding, X., Park, S. I., McCauley, L. K., & Wang, C. Y. (2013). Signaling between transforming growth factor beta (TGF-beta) and transcription factor SNAI2 represses expression of microRNA miR-203 to promote epithelial-mesenchymal transition and tumor metastasis. *J Biol Chem, 288*(15), 10241-10253. doi: 10.1074/jbc.M112.443655

Ding, X. M. (2014). MicroRNAs: regulators of cancer metastasis and epithelial-mesenchymal transition (EMT). *Chin J Cancer, 33*(3), 140-147. doi: 10.5732/cjc.013.10094

Friedl, P., & Gilmour, D. (2009). Collective cell migration in morphogenesis, regeneration and cancer. *Nat Rev Mol Cell Biol, 10*(7), 445-457. doi: 10.1038/nrm2720

Furuta, M., Kozaki, K. I., Tanaka, S., Arii, S., Imoto, I., & Inazawa, J. (2010). miR-124 and miR-203 are epigenetically silenced tumor-suppressive microRNAs in hepatocellular carcinoma. *Carcinogenesis, 31*(5), 766-776. doi: 10.1093/carcin/bgp250

Gao, P., Wang, S., Jing, F., Zhan, J., & Wang, Y. (2017). microRNA-203 suppresses invasion of gastric cancer cells by targeting ERK1/2/Slug/ E-cadherin signaling. *Cancer Biomark, 19*(1), 11-20. doi: 10.3233/CBM-160167

Guttilla, I. K., Adams, B. D., & White, B. A. (2012). ERalpha, microRNAs, and the epithelial-mesenchymal transition in breast cancer. *Trends Endocrinol Metab, 23*(2), 73-82. doi: 10.1016/j.tem.2011.12.001

Heimberg, A. M., Cowper-Sal-lari, R., Semon, M., Donoghue, P. C., & Peterson, K. J. (2010). microRNAs reveal the interrelationships of hagfish, lampreys, and gnathostomes and the nature of the ancestral vertebrate. *Proc Natl Acad Sci U S A, 107*(45), 19379-19383. doi: 10.1073/pnas.1010350107

Hornstein, E., & Shomron, N. (2006). Canalization of development by microRNAs. *Nat Genet, 38 Suppl*, S20-24. doi: 10.1038/ng1803

Hu, N., Strobl-Mazzulla, P., Sauka-Spengler, T., & Bronner, M. E. (2012). DNA methyltransferase3A as a molecular switch mediating the neural tube-to-neural crest fate transition. *Genes Dev, 26*(21), 2380-2385. doi: 10.1101/gad.198747.112

Hu, N., Strobl-Mazzulla, P. H., Simoes-Costa, M., Sanchez-Vasquez, E., & Bronner, M. E. (2014). DNA methyltransferase 3B regulates duration of neural crest production via repression of Sox10. *Proc Natl Acad Sci U S A, 111*(50), 17911-17916. doi: 10.1073/pnas.1318408111

Huang, Y. W., Kuo, C. T., Chen, J. H., Goodfellow, P. J., Huang, T. H., Rader, J. S., & Uyar, D. S. (2014). Hypermethylation of miR-203 in endometrial carcinomas. *Gynecol Oncol, 133*(2), 340-345. doi: 10.1016/j.ygyno.2014.02.009

Ju, S. Y., Chiou, S. H., & Su, Y. (2014). Maintenance of the stemness in CD44(+) HCT-15 and HCT-116 human colon cancer cells requires miR-203 suppression. *Stem Cell Res, 12*(1), 86-100. doi: 10.1016/j.scr.2013.09.011

Kerosuo, L., & Bronner-Fraser, M. (2012). What is bad in cancer is good in the embryo: importance of EMT in neural crest development. *Semin Cell Dev Biol, 23*(3), 320-332. doi: 10.1016/j.semcdb.2012.03.010

Kiesslich, T., Pichler, M., & Neureiter, D. (2013). Epigenetic control of epithelial-mesenchymal-transition in human cancer. *Mol Clin Oncol, 1*(1), 3-11. doi: 10.3892/mco.2012.28

Kloosterman, W. P., & Plasterk, R. H. (2006). The diverse functions of microRNAs in animal development and disease. *Dev Cell, 11*(4), 441-450. doi: 10.1016/j.devcel.2006.09.009

Kluiver, J., Gibcus, J. H., Hettinga, C., Adema, A., Richter, M. K., Halsema, N., . . . van den Berg, A. (2012). Rapid generation of microRNA sponges for microRNA inhibition. *PLoS One, 7*(1), e29275. doi: 10.1371/journal.pone.0029275

Lardizabal, M. N., Nocito, A. L., Daniele, S. M., Ornella, L. A., Palatnik, J. F., & Veggi, L. M. (2012). Reference genes for real-time PCR quantification of microRNAs and messenger RNAs in rat models of hepatotoxicity. *PLoS One, 7*(5), e36323. doi: 10.1371/journal.pone.0036323

Lohcharoenkal, W., Das Mahapatra, K., Pasquali, L., Crudden, C., Kular, L., Akkaya Ulum, Y. Z., . . . Pivarcsi, A. (2018). Genome-Wide Screen for MicroRNAs Reveals a Role for miR-203 in Melanoma Metastasis. *J Invest Dermatol, 138*(4), 882-892. doi: 10.1016/j.jid.2017.09.049

Lujambio, A., Calin, G. A., Villanueva, A., Ropero, S., Sanchez-Cespedes, M., Blanco, D., . . . Esteller, M. (2008). A microRNA DNA methylation signature for human cancer metastasis. *Proc Natl Acad Sci U S A, 105*(36), 13556-13561. doi: 10.1073/pnas.0803055105

Mayor, R., & Theveneau, E. (2013). The neural crest. *Development, 140*(11), 2247-2251. doi: 10.1242/dev.091751

Miao, L., Xiong, X., Lin, Y., Cheng, Y., Lu, J., Zhang, J., & Cheng, N. (2014). miR-203 inhibits tumor cell migration and invasion via caveolin-1 in pancreatic cancer cells. *Oncol Lett, 7*(3), 658-662. doi: 10.3892/ol.2014.1807

Moes, M., Le Bechec, A., Crespo, I., Laurini, C., Halavatyi, A., Vetter, G., . . . Friederich, E. (2012). A novel network integrating a miRNA-203/SNAI1

580 feedback loop which regulates epithelial to mesenchymal transition.
581 *PLoS One, 7*(4), e35440. doi: 10.1371/journal.pone.0035440
582 Nelson, K. M., & Weiss, G. J. (2008). MicroRNAs and cancer: past, present,
583 and potential future. *Mol Cancer Ther, 7*(12), 3655-3660. doi:
584 10.1158/1535-7163.MCT-08-0586
585 Sauka-Spengler, T., & Barembaum, M. (2008). Chapter 12 Gain- and
586 Loss-of-Function Approaches in the Chick Embryo. *87*, 237-256. doi:
587 10.1016/s0091-679x(08)00212-4
588 Scarpa, E., & Mayor, R. (2016). Collective cell migration in development. *J Cell*
589 *Biol, 212*(2), 143-155. doi: 10.1083/jcb.201508047
590 Shi, Y., Tan, Y. J., Zeng, D. Z., Qian, F., & Yu, P. W. (2015). miR-203
591 suppression in gastric carcinoma promotes Slug-mediated cancer
592 metastasis. *Tumour Biol*. doi: 10.1007/s13277-015-3765-8
593 Siegfried, Z., & Simon, I. (2010). DNA methylation and gene expression. *Wiley*
594 *Interdiscip Rev Syst Biol Med, 2*(3), 362-371. doi: 10.1002/wsbm.64
595 Simoes-Costa, M., & Bronner, M. E. (2015). Establishing neural crest identity: a
596 gene regulatory recipe. *Development, 142*(2), 242-257. doi:
597 10.1242/dev.105445
598 Simoes-Costa, M., & Bronner, M. E. (2016). Reprogramming of avian neural
599 crest axial identity and cell fate. *Science, 352*(6293), 1570-1573. doi:
600 10.1126/science.aaf2729
601 Strobl-Mazzulla, P. H., & Bronner, M. E. (2012). A PHD12-Snail2 repressive
602 complex epigenetically mediates neural crest epithelial-to-mesenchymal
603 transition. *J Cell Biol, 198*(6), 999-1010. doi: 10.1083/jcb.201203098
604 Strobl-Mazzulla, P. H., Sauka-Spengler, T., & Bronner-Fraser, M. (2010).
605 Histone demethylase JmjD2A regulates neural crest specification. *Dev*
606 *Cell, 19*(3), 460-468. doi: 10.1016/j.devcel.2010.08.009
607 Taneyhill, L. A., Coles, E. G., & Bronner-Fraser, M. (2007). Snail2 directly
608 represses cadherin6B during epithelial-to-mesenchymal transitions of the
609 neural crest. *Development, 134*(8), 1481-1490. doi: 10.1242/dev.02834
610 Taube, J. H., Malouf, G. G., Lu, E., Sphyris, N., Vijay, V., Ramachandran, P. P.,
611 . . . Mani, S. A. (2013). Epigenetic silencing of microRNA-203 is required
612 for EMT and cancer stem cell properties. *Sci Rep, 3*, 2687. doi:
613 10.1038/srep02687
614 Wang, X., Zhao, J., Huang, J., Tang, H., Yu, S., & Chen, Y. (2012). The
615 regulatory roles of miRNA and methylation on oncogene and tumor
616 suppressor gene expression in pancreatic cancer cells. *Biochem Biophys*
617 *Res Commun, 425*(1), 51-57. doi: 10.1016/j.bbrc.2012.07.047
618 Weber, B., Stresemann, C., Brueckner, B., & Lyko, F. (2007). Methylation of
619 human microRNA genes in normal and neoplastic cells. *Cell Cycle, 6*(9),
620 1001-1005.
621 Wellner, U., Schubert, J., Burk, U. C., Schmalhofer, O., Zhu, F., Sonntag, A., . .
622 . Brabletz, T. (2009). The EMT-activator ZEB1 promotes tumorigenicity
623 by repressing stemness-inhibiting microRNAs. *Nat Cell Biol, 11*(12),
624 1487-1495. doi: 10.1038/ncb1998
625 Wright, J. A., Richer, J. K., & Goodall, G. J. (2010). microRNAs and EMT in
626 mammary cells and breast cancer. *J Mammary Gland Biol Neoplasia,*
627 *15*(2), 213-223. doi: 10.1007/s10911-010-9183-z
628 Xia, H., & Hui, K. M. (2012). MicroRNAs involved in regulating epithelial-
629 mesenchymal transition and cancer stem cells as molecular targets for

630 cancer therapeutics. *Cancer Gene Ther, 19*(11), 723-730. doi:
631 10.1038/cgt.2012.58
632 Xiao, J. N., Yan, T. H., Yu, R. M., Gao, Y., Zeng, W. L., Lu, S. W., . . . Jiang, J.
633 H. (2017). Long non-coding RNA UCA1 regulates the expression of
634 Snail2 by miR-203 to promote hepatocellular carcinoma progression. *J*
635 *Cancer Res Clin Oncol, 143*(6), 981-990. doi: 10.1007/s00432-017-2370-
636 1
637 Zhang, F., Yang, Z., Cao, M., Xu, Y., Li, J., Chen, X., . . . Zeng, Y. (2014). MiR-
638 203 suppresses tumor growth and invasion and down-regulates MiR-21
639 expression through repressing Ran in esophageal cancer. *Cancer Lett,*
640 *342*(1), 121-129. doi: 10.1016/j.canlet.2013.08.037
641 Zhang, J., Zhou, Y., Wu, Y. J., Li, M. J., Wang, R. J., Huang, S. Q., . . . Zhang,
642 J. (2013). Hyper-methylated miR-203 dysregulates ABL1 and contributes
643 to the nickel-induced tumorigenesis. *Toxicol Lett, 223*(1), 42-51. doi:
644 10.1016/j.toxlet.2013.08.007
645 Zhang, K., Dai, L., Zhang, B., Xu, X., Shi, J., Fu, L., . . . Bai, Y. (2015). miR-203
646 Is a Direct Transcriptional Target of E2F1 and Causes G1 Arrest in
647 Esophageal Cancer Cells. *J Cell Physiol, 230*(4), 903-910. doi:
648 10.1002/jcp.24821
649 Zhang, Z., Zhang, B., Li, W., Fu, L., Fu, L., Zhu, Z., & Dong, J. T. (2011).
650 Epigenetic Silencing of miR-203 Upregulates SNAI2 and Contributes to
651 the Invasiveness of Malignant Breast Cancer Cells. *Genes Cancer, 2*(8),
652 782-791. doi: 10.1177/1947601911429743
653 Zhao, S., Yao, D. S., Chen, J. Y., & Ding, N. (2013). Aberrant expression of
654 miR-20a and miR-203 in cervical cancer. *Asian Pac J Cancer Prev,*
655 *14*(4), 2289-2293.
656 Zhu, X., Er, K., Mao, C., Yan, Q., Xu, H., Zhang, Y., . . . Shi, H. (2013). miR-203
657 suppresses tumor growth and angiogenesis by targeting VEGFA in
658 cervical cancer. *Cell Physiol Biochem, 32*(1), 64-73. doi:
659 10.1159/000350125
660

661

Supplemental materials

Figure S1. (A) Whole-mount *in situ* hybridization using DIG-labeled LNA probes (Exiqon) against miR-203 at early chick developmental stages.

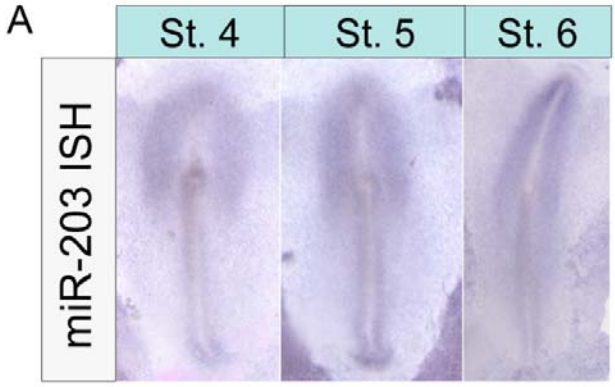

Figure S2: (A) Diagram of electroporation assay for gain-of-function experiments. pCAG-miR-203 does not have a fluorescent marker, for this reason, was co-electroporated with a fluorescent vector that express GFP downstream the CAG promoter. We injected the vectors in the right side of the embryos at stage 4. Following injection, embryos were electroporated and cultured until stage 9. (B) Electroporation of pCAG-203 vector (right side) successfully overexpress a mature miR-203 evidenced by *in situ* hybridization using LNA probes. (C) Schematic drawing of the miRNA dual-sensor vector (pSdmiR-203) containing two copies of complementary sequences to the mature miR-203. (D) Illustration of bilateral electroporation assay to evaluate if pCAG-203 express a functional miR-203. (E) Co-electroporation pSdmiR-203 and the empty pCAG vector (left side) caused that most of the cells are yellow because of the expression of both green and red reporters. Whereas, co-electroporation pSdmiR-203 and pCAG-203 vector (right side) caused that most of the cells are only red, because of the strong repression of the green reporter. pCAG, Chick β-actin promoter; d4EGFP$_N$ nuclear-localized destabilized EGFP with a half-life of 4 h; mRFP$_N$, nuclear-localized monomeric red fluorescent protein.

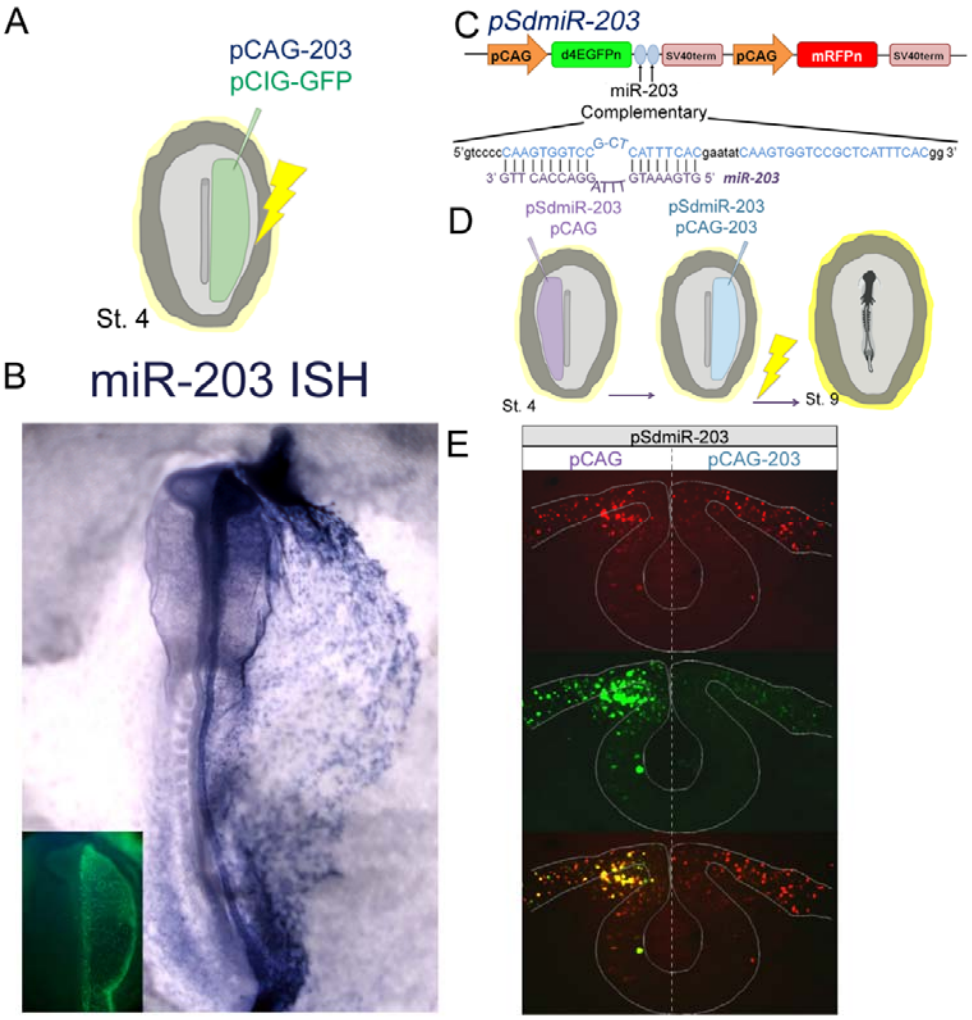

688 **Supplementary table 1:** *In silico* analyzes of conserved and poorly conserved
689 microRNA-binding sites on Snail2 and Phf12 3'UTRs (TargetScan), their known
690 functions, demonstrated targets, and chick expression (GEISHA).
691 **GEISHA microRNAs expression in chick development**
692 http://geisha.arizona.edu/geisha/quick_search.jsp?table=mir
693 **miR-1** (Wei et al., 2014, Wystub et al., 2013, Heidersbach et al., 2013)
694 **miR-19** (Olive et al., 2009, Mavrakis et al., 2010, Liu et al., 2011)
695 **miR32-5p/92-3p/367** (Zhu et al., 2013a, Zhu et al., 2015, Sharifi and Salehi,
696 2016)
697 **miR-33-5p** (Mi et al., 2016, Wang et al., 2016)
698 **miR130-3p/301-3p/454-3p** (Leone et al., 2015, Xia et al., 2015, Lv et al., 2016,
699 Egawa et al., 2016)
700 **miR-142** (Lu et al., 2013, Borges et al., 2016, Sonda et al., 2013, Dickman et
701 al., 2017)
702 **miR-155** (Robertson et al., 2014, Gracias et al., 2013, Forzati et al., 2017)
703 **miR-181-5p** (Ma et al., 2015, Li et al., 2015, Korhan et al., 2014)
704 **miR-200b-3p/429-3p** (Gui et al., 2017, Ye et al., 2014, Wu et al., 2016)
705 **miR-203**(Wei et al., 2010, Yi et al., 2008, Zhang et al., 2011, Shi et al., 2015,
706 Benaich et al., 2014)
707 **miR-221-3p/222-3p** (Yan et al., 2016, Takigawa et al., 2016, Wu et al., 2017)
708 **miR-365-3p** (Wang et al., 2013, Gastaldi et al., 2014)
709 **miR-455-5p** (Liu et al., 2016, Li et al., 2016, Chai et al., 2015)
710
711 ACLOQUE, H., WILKINSON, D. G. & NIETO, M. A. 2008. In situ hybridization
712 analysis of chick embryos in whole-mount and tissue sections. *Methods*
713 *Cell Biol,* 87**,** 169-85.
714 AHMAD, A., LI, Y., BAO, B., KONG, D. & SARKAR, F. H. 2014. Epigenetic
715 regulation of miRNA-cancer stem cells nexus by nutraceuticals. *Mol Nutr*
716 *Food Res,* 58**,** 79-86.
717 BENAICH, N., WOODHOUSE, S., GOLDIE, S. J., MISHRA, A., QUIST, S. R. &
718 WATT, F. M. 2014. Rewiring of an epithelial differentiation factor, miR-
719 203, to inhibit human squamous cell carcinoma metastasis. *Cell Rep,* 9**,**
720 104-17.
721 BOLDRUP, L., COATES, P. J., WAHLGREN, M., LAURELL, G. & NYLANDER,
722 K. 2012. Subsite-based alterations in miR-21, miR-125b, and miR-203 in
723 squamous cell carcinoma of the oral cavity and correlation to important
724 target proteins. *J Carcinog,* 11**,** 18.
725 BOLL, K., REICHE, K., KASACK, K., MORBT, N., KRETZSCHMAR, A. K.,
726 TOMM, J. M., VERHAEGH, G., SCHALKEN, J., VON BERGEN, M.,
727 HORN, F. & HACKERMULLER, J. 2013. MiR-130a, miR-203 and miR-
728 205 jointly repress key oncogenic pathways and are downregulated in
729 prostate carcinoma. *Oncogene,* 32**,** 277-85.
730 BONNOMET, A., BRYSSE, A., TACHSIDIS, A., WALTHAM, M., THOMPSON,
731 E. W., POLETTE, M. & GILLES, C. 2010. Epithelial-to-mesenchymal
732 transitions and circulating tumor cells. *J Mammary Gland Biol Neoplasia,*
733 15**,** 261-73.
734 BORGES, E., JR., SETTI, A. S., BRAGA, D. P., GERALDO, M. V., FIGUEIRA,
735 R. C. & IACONELLI, A., JR. 2016. miR-142-3p as a biomarker of
736 blastocyst implantation failure - A pilot study. *JBRA Assist Reprod,* 20**,**
737 200-205.

738 BU, P. & YANG, P. 2014. MicroRNA-203 inhibits malignant melanoma cell
739 migration by targeting versican. *Exp Ther Med,* 8**,** 309-315.
740 CAO, X., PFAFF, S. L. & GAGE, F. H. 2007. A functional study of miR-124 in
741 the developing neural tube. *Genes Dev,* 21**,** 531-6.
742 CRANE, J. F. & TRAINOR, P. A. 2006. Neural crest stem and progenitor cells.
743 *Annu Rev Cell Dev Biol,* 22**,** 267-86.
744 CHAI, J., WANG, S., HAN, D., DONG, W., XIE, C. & GUO, H. 2015. MicroRNA-
745 455 inhibits proliferation and invasion of colorectal cancer by targeting
746 RAF proto-oncogene serine/threonine-protein kinase. *Tumour Biol,* 36**,**
747 1313-21.
748 CHEN, C., RIDZON, D. A., BROOMER, A. J., ZHOU, Z., LEE, D. H., NGUYEN,
749 J. T., BARBISIN, M., XU, N. L., MAHUVAKAR, V. R., ANDERSEN, M.
750 R., LAO, K. Q., LIVAK, K. J. & GUEGLER, K. J. 2005. Real-time
751 quantification of microRNAs by stem-loop RT-PCR. *Nucleic Acids Res,*
752 33**,** e179.
753 CHEN, H. Y., HAN, Z. B., FAN, J. W., XIA, J., WU, J. Y., QIU, G. Q., TANG, H.
754 M. & PENG, Z. H. 2012. miR-203 expression predicts outcome after liver
755 transplantation for hepatocellular carcinoma in cirrhotic liver. *Med Oncol,*
756 29**,** 1859-65.
757 CHIANG, Y., SONG, Y., WANG, Z., CHEN, Y., YUE, Z., XU, H., XING, C. &
758 LIU, Z. 2011. Aberrant expression of miR-203 and its clinical significance
759 in gastric and colorectal cancers. *J Gastrointest Surg,* 15**,** 63-70.
760 CHIM, C. S., WAN, T. S., WONG, K. Y., FUNG, T. K., DREXLER, H. G. &
761 WONG, K. F. 2011a. Methylation of miR-34a, miR-34b/c, miR-124-1 and
762 miR-203 in Ph-negative myeloproliferative neoplasms. *J Transl Med,* 9**,**
763 197.
764 CHIM, C. S., WONG, K. Y., LEUNG, C. Y., CHUNG, L. P., HUI, P. K., CHAN, S.
765 Y. & YU, L. 2011b. Epigenetic inactivation of the hsa-miR-203 in
766 haematological malignancies. *J Cell Mol Med,* 15**,** 2760-7.
767 DARNELL, D. K., KAUR, S., STANISLAW, S., KONIECZKA, J. H.,
768 YATSKIEVYCH, T. A. & ANTIN, P. B. 2006. MicroRNA expression during
769 chick embryo development. *Dev Dyn,* 235**,** 3156-65.
770 DIAO, Y., GUO, X., JIANG, L., WANG, G., ZHANG, C., WAN, J., JIN, Y. & WU,
771 Z. 2014. miR-203, a tumor suppressor frequently down-regulated by
772 promoter hypermethylation in rhabdomyosarcoma. *J Biol Chem,* 289**,**
773 529-39.
774 DIAZ-LOPEZ, A., MORENO-BUENO, G. & CANO, A. 2014. Role of microRNA
775 in epithelial to mesenchymal transition and metastasis and clinical
776 perspectives. *Cancer Manag Res,* 6**,** 205-16.
777 DICKMAN, C. T., LAWSON, J., JABALEE, J., MACLELLAN, S. A., LEPARD, N.
778 E., BENNEWITH, K. L. & GARNIS, C. 2017. Selective extracellular
779 vesicle exclusion of miR-142-3p by oral cancer cells promotes both
780 internal and extracellular malignant phenotypes. *Oncotarget*.
781 DING, X., PARK, S. I., MCCAULEY, L. K. & WANG, C. Y. 2013. Signaling
782 between transforming growth factor beta (TGF-beta) and transcription
783 factor SNAI2 represses expression of microRNA miR-203 to promote
784 epithelial-mesenchymal transition and tumor metastasis. *J Biol Chem,*
785 288**,** 10241-53.
786 DING, X. M. 2014. MicroRNAs: regulators of cancer metastasis and epithelial-
787 mesenchymal transition (EMT). *Chin J Cancer,* 33**,** 140-7.

EGAWA, H., JINGUSHI, K., HIRONO, T., UEDA, Y., KITAE, K., NAKATA, W., FUJITA, K., UEMURA, M., NONOMURA, N. & TSUJIKAWA, K. 2016. The miR-130 family promotes cell migration and invasion in bladder cancer through FAK and Akt phosphorylation by regulating PTEN. *Sci Rep,* 6**,** 20574.

FORZATI, F., DE MARTINO, M., ESPOSITO, F., SEPE, R., PELLECCHIA, S., MALAPELLE, U., PELLINO, G., ARRA, C. & FUSCO, A. 2017. miR-155 is positively regulated by CBX7 in mouse embryonic fibroblasts and colon carcinomas, and targets the KRAS oncogene. *BMC Cancer,* 17**,** 170.

FRIEDL, P. & GILMOUR, D. 2009. Collective cell migration in morphogenesis, regeneration and cancer. *Nat Rev Mol Cell Biol,* 10**,** 445-57.

FURUTA, M., KOZAKI, K. I., TANAKA, S., ARII, S., IMOTO, I. & INAZAWA, J. 2010. miR-124 and miR-203 are epigenetically silenced tumor-suppressive microRNAs in hepatocellular carcinoma. *Carcinogenesis,* 31**,** 766-76.

GAO, P., WANG, S., JING, F., ZHAN, J. & WANG, Y. 2017. microRNA-203 suppresses invasion of gastric cancer cells by targeting ERK1/2/Slug/ E-cadherin signaling. *Cancer Biomark,* 19**,** 11-20.

GASTALDI, C., BERTERO, T., XU, N., BOURGET-PONZIO, I., LEBRIGAND, K., FOURRE, S., POPA, A., CARDOT-LECCIA, N., MENEGUZZI, G., SONKOLY, E., PIVARCSI, A., MARI, B., BARBRY, P., PONZIO, G. & REZZONICO, R. 2014. miR-193b/365a cluster controls progression of epidermal squamous cell carcinoma. *Carcinogenesis,* 35**,** 1110-20.

GRACIAS, D. T., STELEKATI, E., HOPE, J. L., BOESTEANU, A. C., DOERING, T. A., NORTON, J., MUELLER, Y. M., FRAIETTA, J. A., WHERRY, E. J., TURNER, M. & KATSIKIS, P. D. 2013. The microRNA miR-155 controls CD8(+) T cell responses by regulating interferon signaling. *Nat Immunol,* 14**,** 593-602.

GUI, Z., LUO, F., YANG, Y., SHEN, C., LI, S. & XU, J. 2017. Oridonin inhibition and miR200b3p/ZEB1 axis in human pancreatic cancer. *Int J Oncol,* 50**,** 111-120.

GUTTILLA, I. K., ADAMS, B. D. & WHITE, B. A. 2012. ERalpha, microRNAs, and the epithelial-mesenchymal transition in breast cancer. *Trends Endocrinol Metab,* 23**,** 73-82.

HEIDERSBACH, A., SAXBY, C., CARVER-MOORE, K., HUANG, Y., ANG, Y. S., DE JONG, P. J., IVEY, K. N. & SRIVASTAVA, D. 2013. microRNA-1 regulates sarcomere formation and suppresses smooth muscle gene expression in the mammalian heart. *Elife,* 2**,** e01323.

HEIMBERG, A. M., COWPER-SAL-LARI, R., SEMON, M., DONOGHUE, P. C. & PETERSON, K. J. 2010. microRNAs reveal the interrelationships of hagfish, lampreys, and gnathostomes and the nature of the ancestral vertebrate. *Proc Natl Acad Sci U S A,* 107**,** 19379-83.

HORNSTEIN, E. & SHOMRON, N. 2006. Canalization of development by microRNAs. *Nat Genet,* 38 Suppl**,** S20-4.

HU, N., STROBL-MAZZULLA, P., SAUKA-SPENGLER, T. & BRONNER, M. E. 2012. DNA methyltransferase3A as a molecular switch mediating the neural tube-to-neural crest fate transition. *Genes Dev,* 26**,** 2380-5.

HU, N., STROBL-MAZZULLA, P. H., SIMOES-COSTA, M., SANCHEZ-VASQUEZ, E. & BRONNER, M. E. 2014. DNA methyltransferase 3B

regulates duration of neural crest production via repression of Sox10. *Proc Natl Acad Sci U S A,* 111**,** 17911-6.

HUANG, Y. W., KUO, C. T., CHEN, J. H., GOODFELLOW, P. J., HUANG, T. H., RADER, J. S. & UYAR, D. S. 2014. Hypermethylation of miR-203 in endometrial carcinomas. *Gynecol Oncol,* 133**,** 340-5.

JU, S. Y., CHIOU, S. H. & SU, Y. 2014. Maintenance of the stemness in CD44(+) HCT-15 and HCT-116 human colon cancer cells requires miR-203 suppression. *Stem Cell Res,* 12**,** 86-100.

KEROSUO, L. & BRONNER-FRASER, M. 2012. What is bad in cancer is good in the embryo: importance of EMT in neural crest development. *Semin Cell Dev Biol,* 23**,** 320-32.

KIESSLICH, T., PICHLER, M. & NEUREITER, D. 2013. Epigenetic control of epithelial-mesenchymal-transition in human cancer. *Mol Clin Oncol,* 1**,** 3-11.

KLOOSTERMAN, W. P. & PLASTERK, R. H. 2006. The diverse functions of microRNAs in animal development and disease. *Dev Cell,* 11**,** 441-50.

KLUIVER, J., GIBCUS, J. H., HETTINGA, C., ADEMA, A., RICHTER, M. K., HALSEMA, N., SLEZAK-PROCHAZKA, I., DING, Y., KROESEN, B. J. & VAN DEN BERG, A. 2012. Rapid generation of microRNA sponges for microRNA inhibition. *PLoS One,* 7**,** e29275.

KORHAN, P., ERDAL, E. & ATABEY, N. 2014. MiR-181a-5p is downregulated in hepatocellular carcinoma and suppresses motility, invasion and branching-morphogenesis by directly targeting c-Met. *Biochem Biophys Res Commun,* 450**,** 1304-12.

LARDIZABAL, M. N., NOCITO, A. L., DANIELE, S. M., ORNELLA, L. A., PALATNIK, J. F. & VEGGI, L. M. 2012. Reference genes for real-time PCR quantification of microRNAs and messenger RNAs in rat models of hepatotoxicity. *PLoS One,* 7**,** e36323.

LEONE, V., LANGELLA, C., ESPOSITO, F., DE MARTINO, M., DECAUSSIN-PETRUCCI, M., CHIAPPETTA, G., BIANCO, A. & FUSCO, A. 2015. miR-130b-3p Upregulation Contributes to the Development of Thyroid Adenomas Targeting CCDC6 Gene. *Eur Thyroid J,* 4**,** 213-21.

LI, Y., KUSCU, C., BANACH, A., ZHANG, Q., PULKOSKI-GROSS, A., KIM, D., LIU, J., ROTH, E., LI, E., SHROYER, K. R., DENOYA, P. I., ZHU, X., CHEN, L. & CAO, J. 2015. miR-181a-5p Inhibits Cancer Cell Migration and Angiogenesis via Downregulation of Matrix Metalloproteinase-14. *Cancer Res,* 75**,** 2674-85.

LI, Y. J., PING, C., TANG, J. & ZHANG, W. 2016. MicroRNA-455 suppresses non-small cell lung cancer through targeting ZEB1. *Cell Biol Int,* 40**,** 621-8.

LIU, J., ZHANG, J., LI, Y., WANG, L., SUI, B. & DAI, D. 2016. MiR-455-5p acts as a novel tumor suppressor in gastric cancer by down-regulating RAB18. *Gene,* 592**,** 308-15.

LIU, M., WANG, Z., YANG, S., ZHANG, W., HE, S., HU, C., ZHU, H., QUAN, L., BAI, J. & XU, N. 2011. TNF-alpha is a novel target of miR-19a. *Int J Oncol,* 38**,** 1013-22.

LOHCHAROENKAL, W., DAS MAHAPATRA, K., PASQUALI, L., CRUDDEN, C., KULAR, L., AKKAYA ULUM, Y. Z., ZHANG, L., XU LANDEN, N., GIRNITA, L., JAGODIC, M., STAHLE, M., SONKOLY, E. & PIVARCSI,

A. 2018. Genome-Wide Screen for MicroRNAs Reveals a Role for miR-203 in Melanoma Metastasis. *J Invest Dermatol,* 138**,** 882-892.

LU, X., LI, X., HE, Q., GAO, J., GAO, Y., LIU, B. & LIU, F. 2013. miR-142-3p regulates the formation and differentiation of hematopoietic stem cells in vertebrates. *Cell Res,* 23**,** 1356-68.

LUJAMBIO, A., CALIN, G. A., VILLANUEVA, A., ROPERO, S., SANCHEZ-CESPEDES, M., BLANCO, D., MONTUENGA, L. M., ROSSI, S., NICOLOSO, M. S., FALLER, W. J., GALLAGHER, W. M., ECCLES, S. A., CROCE, C. M. & ESTELLER, M. 2008. A microRNA DNA methylation signature for human cancer metastasis. *Proc Natl Acad Sci U S A,* 105**,** 13556-61.

LV, M., ZHONG, Z., CHI, H., HUANG, M., JIANG, R. & CHEN, J. 2016. Genome-Wide Screen of miRNAs and Targeting mRNAs Reveals the Negatively Regulatory Effect of miR-130b-3p on PTEN by PI3K and Integrin beta1 Signaling Pathways in Bladder Carcinoma. *Int J Mol Sci,* 18.

MA, Z., QIU, X., WANG, D., LI, Y., ZHANG, B., YUAN, T., WEI, J., ZHAO, B., ZHAO, X., LOU, J., JIN, Y. & JIN, Y. 2015. MiR-181a-5p inhibits cell proliferation and migration by targeting Kras in non-small cell lung cancer A549 cells. *Acta Biochim Biophys Sin (Shanghai),* 47**,** 630-8.

MAVRAKIS, K. J., WOLFE, A. L., ORICCHIO, E., PALOMERO, T., DE KEERSMAECKER, K., MCJUNKIN, K., ZUBER, J., JAMES, T., KHAN, A. A., LESLIE, C. S., PARKER, J. S., PADDISON, P. J., TAM, W., FERRANDO, A. & WENDEL, H. G. 2010. Genome-wide RNA-mediated interference screen identifies miR-19 targets in Notch-induced T-cell acute lymphoblastic leukaemia. *Nat Cell Biol,* 12**,** 372-9.

MAYOR, R. & THEVENEAU, E. 2013. The neural crest. *Development,* 140**,** 2247-51.

MI, W., SHI, Q., CHEN, X., WU, T. & HUANG, H. 2016. miR-33a-5p modulates TNF-alpha-inhibited osteogenic differentiation by targeting SATB2 expression in hBMSCs. *FEBS Lett,* 590**,** 396-407.

MIAO, L., XIONG, X., LIN, Y., CHENG, Y., LU, J., ZHANG, J. & CHENG, N. 2014. miR-203 inhibits tumor cell migration and invasion via caveolin-1 in pancreatic cancer cells. *Oncol Lett,* 7**,** 658-662.

MOES, M., LE BECHEC, A., CRESPO, I., LAURINI, C., HALAVATYI, A., VETTER, G., DEL SOL, A. & FRIEDERICH, E. 2012. A novel network integrating a miRNA-203/SNAI1 feedback loop which regulates epithelial to mesenchymal transition. *PLoS One,* 7**,** e35440.

NELSON, K. M. & WEISS, G. J. 2008. MicroRNAs and cancer: past, present, and potential future. *Mol Cancer Ther,* 7**,** 3655-60.

OLIVE, V., BENNETT, M. J., WALKER, J. C., MA, C., JIANG, I., CORDON-CARDO, C., LI, Q. J., LOWE, S. W., HANNON, G. J. & HE, L. 2009. miR-19 is a key oncogenic component of mir-17-92. *Genes Dev,* 23**,** 2839-49.

ROBERTSON, E. D., WASYLYK, C., YE, T., JUNG, A. C. & WASYLYK, B. 2014. The oncogenic MicroRNA Hsa-miR-155-5p targets the transcription factor ELK3 and links it to the hypoxia response. *PLoS One,* 9**,** e113050.

SAUKA-SPENGLER, T. & BAREMBAUM, M. 2008. Chapter 12 Gain- and Loss-of-Function Approaches in the Chick Embryo. 87**,** 237-256.

SCARPA, E. & MAYOR, R. 2016. Collective cell migration in development. *J Cell Biol,* 212**,** 143-55.

SHARIFI, M. & SALEHI, R. 2016. Blockage of miR-92a-3p with locked nucleic acid induces apoptosis and prevents cell proliferation in human acute megakaryoblastic leukemia. *Cancer Gene Ther,* 23**,** 29-35.

SHI, Y., TAN, Y. J., ZENG, D. Z., QIAN, F. & YU, P. W. 2015. miR-203 suppression in gastric carcinoma promotes Slug-mediated cancer metastasis. *Tumour Biol*.

SIEGFRIED, Z. & SIMON, I. 2010. DNA methylation and gene expression. *Wiley Interdiscip Rev Syst Biol Med,* 2**,** 362-371.

SIMOES-COSTA, M. & BRONNER, M. E. 2015. Establishing neural crest identity: a gene regulatory recipe. *Development,* 142**,** 242-57.

SIMOES-COSTA, M. & BRONNER, M. E. 2016. Reprogramming of avian neural crest axial identity and cell fate. *Science,* 352**,** 1570-3.

SONDA, N., SIMONATO, F., PERANZONI, E., CALI, B., BORTOLUZZI, S., BISOGNIN, A., WANG, E., MARINCOLA, F. M., NALDINI, L., GENTNER, B., TRAUTWEIN, C., SACKETT, S. D., ZANOVELLO, P., MOLON, B. & BRONTE, V. 2013. miR-142-3p prevents macrophage differentiation during cancer-induced myelopoiesis. *Immunity,* 38**,** 1236-49.

STROBL-MAZZULLA, P. H. & BRONNER, M. E. 2012. A PHD12-Snail2 repressive complex epigenetically mediates neural crest epithelial-to-mesenchymal transition. *J Cell Biol,* 198**,** 999-1010.

STROBL-MAZZULLA, P. H., SAUKA-SPENGLER, T. & BRONNER-FRASER, M. 2010. Histone demethylase JmjD2A regulates neural crest specification. *Dev Cell,* 19**,** 460-8.

TAKIGAWA, S., CHEN, A., WAN, Q., NA, S., SUDO, A., YOKOTA, H. & HAMAMURA, K. 2016. Role of miR-222-3p in c-Src-Mediated Regulation of Osteoclastogenesis. *Int J Mol Sci,* 17**,** 240.

TANEYHILL, L. A., COLES, E. G. & BRONNER-FRASER, M. 2007. Snail2 directly represses cadherin6B during epithelial-to-mesenchymal transitions of the neural crest. *Development,* 134**,** 1481-90.

TAUBE, J. H., MALOUF, G. G., LU, E., SPHYRIS, N., VIJAY, V., RAMACHANDRAN, P. P., UENO, K. R., GAUR, S., NICOLOSO, M. S., ROSSI, S., HERSCHKOWITZ, J. I., ROSEN, J. M., ISSA, J. P., CALIN, G. A., CHANG, J. T. & MANI, S. A. 2013. Epigenetic silencing of microRNA-203 is required for EMT and cancer stem cell properties. *Sci Rep,* 3**,** 2687.

WANG, H., SUN, Z., WANG, Y., HU, Z., ZHOU, H., ZHANG, L., HONG, B., ZHANG, S. & CAO, X. 2016. miR-33-5p, a novel mechano-sensitive microRNA promotes osteoblast differentiation by targeting Hmga2. *Sci Rep,* 6**,** 23170.

WANG, J., WANG, X., WU, G., HOU, D. & HU, Q. 2013. MiR-365b-3p, down-regulated in retinoblastoma, regulates cell cycle progression and apoptosis of human retinoblastoma cells by targeting PAX6. *FEBS Lett,* 587**,** 1779-86.

WANG, X., ZHAO, J., HUANG, J., TANG, H., YU, S. & CHEN, Y. 2012. The regulatory roles of miRNA and methylation on oncogene and tumor suppressor gene expression in pancreatic cancer cells. *Biochem Biophys Res Commun,* 425**,** 51-7.

WEBER, B., STRESEMANN, C., BRUECKNER, B. & LYKO, F. 2007. Methylation of human microRNA genes in normal and neoplastic cells. *Cell Cycle,* 6**,** 1001-5.

WEI, T., ORFANIDIS, K., XU, N., JANSON, P., STAHLE, M., PIVARCSI, A. & SONKOLY, E. 2010. The expression of microRNA-203 during human skin morphogenesis. *Exp Dermatol,* 19**,** 854-6.

WEI, Y., PENG, S., WU, M., SACHIDANANDAM, R., TU, Z., ZHANG, S., FALCE, C., SOBIE, E. A., LEBECHE, D. & ZHAO, Y. 2014. Multifaceted roles of miR-1s in repressing the fetal gene program in the heart. *Cell Res,* 24**,** 278-92.

WELLNER, U., SCHUBERT, J., BURK, U. C., SCHMALHOFER, O., ZHU, F., SONNTAG, A., WALDVOGEL, B., VANNIER, C., DARLING, D., ZUR HAUSEN, A., BRUNTON, V. G., MORTON, J., SANSOM, O., SCHULER, J., STEMMLER, M. P., HERZBERGER, C., HOPT, U., KECK, T., BRABLETZ, S. & BRABLETZ, T. 2009. The EMT-activator ZEB1 promotes tumorigenicity by repressing stemness-inhibiting microRNAs. *Nat Cell Biol,* 11**,** 1487-95.

WRIGHT, J. A., RICHER, J. K. & GOODALL, G. J. 2010. microRNAs and EMT in mammary cells and breast cancer. *J Mammary Gland Biol Neoplasia,* 15**,** 213-23.

WU, J., CUI, H., ZHU, Z. & WANG, L. 2016. MicroRNA-200b-3p suppresses epithelial-mesenchymal transition and inhibits tumor growth of glioma through down-regulation of ERK5. *Biochem Biophys Res Commun,* 478**,** 1158-64.

WU, Q., REN, X., ZHANG, Y., FU, X., LI, Y., PENG, Y., XIAO, Q., LI, T., OUYANG, C., HU, Y., ZHANG, Y., ZHOU, W., YAN, W., GUO, K., LI, W., HU, Y., YANG, X., SHU, G., XUE, H., WEI, Z., LUO, Y. & YIN, G. 2017. MiR-221-3p targets ARF4 and inhibits the proliferation and migration of epithelial ovarian cancer cells. *Biochem Biophys Res Commun*.

WYSTUB, K., BESSER, J., BACHMANN, A., BOETTGER, T. & BRAUN, T. 2013. miR-1/133a clusters cooperatively specify the cardiomyogenic lineage by adjustment of myocardin levels during embryonic heart development. *PLoS Genet,* 9**,** e1003793.

XIA, H. & HUI, K. M. 2012. MicroRNAs involved in regulating epithelial-mesenchymal transition and cancer stem cells as molecular targets for cancer therapeutics. *Cancer Gene Ther,* 19**,** 723-30.

XIA, X., ZHANG, K., CEN, G., JIANG, T., CAO, J., HUANG, K., HUANG, C., ZHAO, Q. & QIU, Z. 2015. MicroRNA-301a-3p promotes pancreatic cancer progression via negative regulation of SMAD4. *Oncotarget,* 6**,** 21046-63.

XIAO, J. N., YAN, T. H., YU, R. M., GAO, Y., ZENG, W. L., LU, S. W., QUE, H. X., LIU, Z. P. & JIANG, J. H. 2017. Long non-coding RNA UCA1 regulates the expression of Snail2 by miR-203 to promote hepatocellular carcinoma progression. *J Cancer Res Clin Oncol,* 143**,** 981-990.

YAN, J., GUO, D., YANG, S., SUN, H., WU, B. & ZHOU, D. 2016. Inhibition of miR-222-3p activity promoted osteogenic differentiation of hBMSCs by regulating Smad5-RUNX2 signal axis. *Biochem Biophys Res Commun,* 470**,** 498-503.

YE, F., TANG, H., LIU, Q., XIE, X., WU, M., LIU, X., CHEN, B. & XIE, X. 2014. miR-200b as a prognostic factor in breast cancer targets multiple members of RAB family. *J Transl Med,* 12**,** 17.

YI, R., POY, M. N., STOFFEL, M. & FUCHS, E. 2008. A skin microRNA promotes differentiation by repressing 'stemness'. *Nature,* 452**,** 225-9.

ZHANG, F., YANG, Z., CAO, M., XU, Y., LI, J., CHEN, X., GAO, Z., XIN, J., ZHOU, S., ZHOU, Z., YANG, Y., SHENG, W. & ZENG, Y. 2014. MiR-203 suppresses tumor growth and invasion and down-regulates MiR-21 expression through repressing Ran in esophageal cancer. *Cancer Lett,* 342**,** 121-9.

ZHANG, J., ZHOU, Y., WU, Y. J., LI, M. J., WANG, R. J., HUANG, S. Q., GAO, R. R., MA, L., SHI, H. J. & ZHANG, J. 2013. Hyper-methylated miR-203 dysregulates ABL1 and contributes to the nickel-induced tumorigenesis. *Toxicol Lett,* 223**,** 42-51.

ZHANG, K., DAI, L., ZHANG, B., XU, X., SHI, J., FU, L., CHEN, X., LI, J. & BAI, Y. 2015. miR-203 Is a Direct Transcriptional Target of E2F1 and Causes G1 Arrest in Esophageal Cancer Cells. *J Cell Physiol,* 230**,** 903-10.

ZHANG, Z., ZHANG, B., LI, W., FU, L., FU, L., ZHU, Z. & DONG, J. T. 2011. Epigenetic Silencing of miR-203 Upregulates SNAI2 and Contributes to the Invasiveness of Malignant Breast Cancer Cells. *Genes Cancer,* 2**,** 782-91.

ZHAO, S., YAO, D. S., CHEN, J. Y. & DING, N. 2013. Aberrant expression of miR-20a and miR-203 in cervical cancer. *Asian Pac J Cancer Prev,* 14**,** 2289-93.

ZHU, G., CHAI, J., MA, L., DUAN, H. & ZHANG, H. 2013a. Downregulated microRNA-32 expression induced by high glucose inhibits cell cycle progression via PTEN upregulation and Akt inactivation in bone marrow-derived mesenchymal stem cells. *Biochem Biophys Res Commun,* 433**,** 526-31.

ZHU, X., ER, K., MAO, C., YAN, Q., XU, H., ZHANG, Y., ZHU, J., CUI, F., ZHAO, W. & SHI, H. 2013b. miR-203 suppresses tumor growth and angiogenesis by targeting VEGFA in cervical cancer. *Cell Physiol Biochem,* 32**,** 64-73.

ZHU, Z., XU, Y., ZHAO, J., LIU, Q., FENG, W., FAN, J. & WANG, P. 2015. miR-367 promotes epithelial-to-mesenchymal transition and invasion of pancreatic ductal adenocarcinoma cells by targeting the Smad7-TGF-beta signalling pathway. *Br J Cancer,* 112**,** 1367-75.

		Conserved sites			Poorly conserved sites					Known function	Known Target Gene	Reference	Expression (GEISHA) Stages 3-25
		8mer	7mer-m8	7mer-1A	8mer	7mer-m8	7mer-1A	6mers	Pct				
Phf12	miR-19-3p	1	0	0	0	0	0	1	0,85	Oncogene	Pten,Bim,TNF-α	Olive et al. 2009; Mavrakis et al. 2010; Liu et al. 2011	Broadly expressed but at much reduced levels in the heart
	miR-130-3p /301-3p /454-3p	1	0	0	0	0	0	0	0,77	Oncogene	Coiled-coil domain-containing protein 6 (CCDC6), Smad4, Pten	Leone et al. 2015; Xia et al. 2015; Egawa et al. 2016; Lv et al. 2016	Hindbrain, spinal cord, widespread expression after stage 21 except in heart
	miR-365-3p	0	1	0	0	0	0	1	0,41	Tumor suppressor	KRAS, MAX, PAX6	Wang et al. 2013; Gastaldi et al. 2014	No expression detected until stage 14, extraembryonic, notochord, surface ectoderm, widespread expression after stage 19
	miR-142-3p	0	0	1	0	0	0	0	0,4	Tumor suppressor, hematopoietic development	Interferon regulatory factor 7 (Irf7), interleukin 6 signal transducer (IL6st), transforming growth factor beta receptor 1(TGFBR1)	Lu et al. 2013; Sonda et al. 2013; Borges et al. 2016; Dickman et al. 2017	No expression detected until stage 20, atria, sinus venosus
	miR-455-5p	0	0	1	0	0	0	0	0,38	Tumor suppressor	RAB18, ZEB1, RA F proto-oncogene serine/threonine-protein kinase (RAF1)	Chai et al. 2015; Li et al. 2016; Liu et al. 2016	Unknown
	miR-221-3p /222-3p	0	0	1	0	0	0	0	0,36	Osteoblasts/ osteocytes develop	RUNX2, Smad5, tartrate-resistant acid phosphatase (TRAP), ADP-ribosylation factor 4(ARF4)	Takigawa et al. 2016; Yan et al. 2016; Wu et al. 2017	No expression detected until stage 14, low level ubiquitous from stage 16-25
	miR-33-5p	1	0	0	0	0	0	0	0,32				
	miR-203	0	1	0	0	0	0	0	0,31				
	miR-7467-3p	0	0	1	0	0	0	0	0,24	Unknown	Unknown	Unknown	Unknown
Snai2	miR-1-3p/206	0	1	0	0	1	0	0	0,72	Cardiovascular development	ERβ1, myocardin, telokin	Heidersbach et al. 2013; Wystub et al. 2013; Wei et al. 2014	Atria, heart, myocardium, myotome, somites, ventricles
	miR-181-5p	0	0	1	0	1	0	1	0,47	Tumor suppressor	KRAS,matrix metalloproteinase MMP-14, c-Met	Korhan et al. 2014; Li et al. 2015; Ma et al. 2015	Ubiquitous
	miR-200b-3p /429-3p	0	1	0	0	0	0	1	0,43	Tumor suppressor	Zeb1, multiple members of RAB family, extracellular-regulated protein kina se 5 (ERK5)	Ye et al. 2014; Wu et al. 2016; Gui et al. 2017	Surface ectoderm from stage 13-18, diverse expression before stage 20
	miR-203	1	0	0	0	0	0	1	0,38	Skin development, tumor suppressor	p63, Snail2, LIM and SH3 domain protein 1 (LASP1)	Yi et al. 2008; Wei et al. 2010; Zhang et al. 2011; Benaich et al. 2014; Shi et al. 2015	Ubiquitous after stage 15, no expression detected at stage 5
	miR-33-5p	0	0	1	0	1	0	1	0,31	Osteoblasts/ osteocytes develop	Special AT-rich sequence-binding protein 2 (SATB2), high-mobility group AT-hook 2(HMGA2)	Mi et al. 2016; Wang et al. 2016	No expression detected until stage 21, amnion, atria, extraembryonic
	miR-155	0	0	0	0	1	0	0	0,23	Oncogene	ELK3 (ETS Transcription Factor), several mRNAs	Gracias et al. 2013; Robertson et al. 2014; Forzati et al. 2017	No expression detected stage 3-24
	miR-32-5p /92-3p/367	0	0	0	0	0	1	0	0,22	Oncogene	Pten, Smad7, estrogen-related receptor β (ERβ1)	Zhu et al. 2013; Zhu et al. 2015; Sharifi and Salehi 2016	Neural Plate/Tube, spinal cord, widespread expression

1073

Supplementary table 2: Results obtained with the Jaspar 2018 (http://jaspar.genereg.net/) for SNAIL2 binding site in the tentative promoter of miR-203. High binding sites (>9) are mapped in figure 2A. We also show the sequence analyzed in Jaspar 2018.

Matrix ID	Name	Score	Relative score	Sequence ID	Start	End	Strand	Predicted sequence
MA0745.1	SNAI2	12,6931	0.999707221414	miR_203_tentative_promoter	-1162	-1153	+	AACAGGTGC
MA0745.1	SNAI2	9,71729	0.94034684341	miR_203_tentative_promoter	-1552	-1543	+	GGCAGGTAC
MA0745.1	SNAI2	8,48966	0.915858769456	miR_203_tentative_promoter	-1089	-1080	-	CACAGGTTG
MA0745.1	SNAI2	7,98092	0.905710714071	miR_203_tentative_promoter	-1273	-1264	-	ATCAGGTTG
MA0745.1	SNAI2	4,63965	0.839061031445	miR_203_tentative_promoter	-1599	-1590	-	TGCATGTTT
MA0745.1	SNAI2	3,94346	0.825173896668	miR_203_tentative_promoter	-1527	-1518	+	TCAAGGTGT
MA0745.1	SNAI2	3,5435	0.817195747557	miR_203_tentative_promoter	-1199	-1190	-	TGGAGGTTG
MA0745.1	SNAI2	3,51455	0.816618237138	miR_203_tentative_promoter	-1293	-1284	+	AGAAAGTGA
MA0745.1	SNAI2	3,24005	0.811142584031	miR_203_tentative_promoter	-1082	-1071	+	TGCCAGTGC

>miR_203_tentative_promoter Chr 5:50767590-50768212
AGGACTGGCTTGAGTTGCCTATATATTTATAAAGAGCCAAAGATCATAGGATCTGGAGTGCCAGAATTCATACACAGCACATATACAGCTCTTTAAACATGCAAAACACTCTATTAACATGA
GTGAAGCCTCATAAGATGAGGCAGGTACGCATTATCTCTCCTCCTCAAGGTGTGGCGAAGTGACTTGGTGAAGGCCTGAGGCTGAGTCGCTGGCAGAGCAGGGCCGACTATCCACAACTT
TCCTACACCACACAGGCTGCCCCGTCCCAGCATGGCAAAGCGTGAAGGCCTTCCCGTCCACCCCAGCAGCAGGGCTCCGAAAGCCCAGTGGGTTGTGTTTCATTCTTCTCCTATAGACAAAG
AGGGTGAAATATTAATGGAAGAAAGTCAAAATTCAGAGAAAGTGACTCCCGGCAAGCAACCTGATTTCTGGAAGTTCATGAAATCATACAATTGTTTGAGTTGGAAGGGACCCCTAAAGG
CCATCCAGTCCAACCTCCATGCAATAAGTAGGGACTCCCACGGCTCCAACAGGTGCTCAGAGCCCCGTCCAGCCTGACCTTGGCTGTCTCTAAGGACAGGGCACCCACCACATCTCTGGGCA
ACCTGTGCCAGTGCCTC

Supplementary table 3: Complete list of utilized primers, LNA probe, and morpholinos

Gene/Direction	Sequence
LNA Probe	
dre-miR-203a(gga-miR-203)	CAAGTGGTCCTAAACATTTCAC
RT-qPCR Primer Sequences	
stem-loop-gga-miR-203	GTCTCCTCTGGTGCAGGGTCCGAGGTATTCGCACCAGAGGAGACCAAGTG
stem-loop-gga-miR-16	GTCTCCTCTGGTGCAGGGTCCGAGGTATTCGCACCAGAGGAGACCAAGTG
qPCR-gga-miR-203 Fwd	CCGGCGTGAAATGTTTAGG
qPCR-gga-miR-16 Fwd	CGCCGCTAGCAGCACGTAAA
qPCR-gga-miR-universal Rev	GAGGTATTCGCACCAGAGGA
qPCR-Snail2 Fwd	GCCAAACTACAGCGAACTGG
qPCR-Snail2 Rev	CGGAGAGAGGTCATTGGGTA
qPCR-Phf12-Fwd	CTGAGGAACCCTTGCAGAAG
qPCR-Phf12-Rev	AGAGTCCCAAAGCGAAGTCA
qPCR-HPRT1-Fwd	TGGTGAAAGTGGCCAGTTTG
qPCR-HPRT1-Rev	TCATTGTAGTCGAGGGCGTATC
Bisulfite Primer Sequences	
Proximal region	
P-miR-203 Fwd	AGGTAGTTTGGAAAAATTGGTTT
P-miR_203 Rev	CTCCTTTAAAAACATTACAACCC
PN-miR-203 Fwd	AAGTTTTGTTGTTGTTGTTATTTT
PN-miR-203 Rev	TAAACTATTAAAAACCACTACACCA
Distal region	

D-miR-203 Fwd	TTTATATTTGTTGAGGGGAAGG
D-miR-203 Rev	TTTCCAAACTACCTTCTCCCTA
DN-miR-203 Fwd	TTGTGTGAGGTTGGTAGTTAGG
DN-miR-203 Rev	ATCATCATCATCTAAAACAACCC
pCAG-miR-203 cloning	
XhoI-gga-miR-203 Fwd	AAACTCGAGCTCCGAGCTGAGAAGAATGG
EcoRV-gga-miR-203 Rev	AAAGATATCCGCGCACTACAAGCCTATTT
Sponge cloning	
miR-203 sponge Fwd	gtcccCAAGTGGTCCGCTCATTTCACgaatatCAAGTGGTCCGCTCATTTCACgg
miR-203 sponge Rev	gacccGTGAAATGAGCGGACCACTTGatattcGTGAAATGAGCGGACCACTTGgg
Scramble sponge Fwd	gtcccATCTAGCTGATCTAATCGAACaatatATCTAGCTGATCTAATCGAACgg
Scramble sponge Rev	gacccGTTCGATTAGATCAGCTAGATatattGTTCGATTAGATCAGCTAGATgg
pUTRs cloning	
Snail2-3'UTR Fwd	ACGCGTGTCATGCAGTCAATGTTTAC
Snail2-3'UTR Rev	GCTAGCTTTCACTTCACGCTTTCTTC
mutSnail2-3'UTR SITIO A Fwd	ATGCATGAGACCCGCAGTAGATCTAAACG
mutSnail2-3'UTR SITIO A Rev	GCGGGTCTCATGCATGGCATCTTTCCCC
mutSnail2-3'UTR SITIO B Fwd	CAAGCGACCCGCACCAAAGAAACAGTATTTTAATGG
mutSnail2-3'UTR SITIO B Rev	GGTGCGGGTCGCTTGGCAGGAATGTATTAGTAAC
Phf12-3'UTR SanDI Fwd	AAAGGGTCCCGAATTTGGAGGAAGGGAGCT
Phf12-3'UTR Rev	GCTAGCTACAGTGGAGCTAGCTGGCC
mutPhf12-3'UTR Rev	AAAACGCGTGCTGCTCTCGCTGCAGTTTTCCTTTTAAAAGCGGGTCTATAG
Morpholinos Sequences	
DNMT3A MO	TGGGTGTGTCACTGCTTTCCACCAT
DNMT3B MO	CGAGGCTCGTTACCATGCTCATCGC
SNAIL2 MO	TCTTGACCAG GAAGGAGC